

**AIR CONDITIONAL REFRIGERANT PIPE LEAKAGE LOCATION
IDENTIFICATION USING OPTICAL SENSORS**

JACKY KHO SENG YONG

**A project report submitted in partial fulfilment of the
requirements for the award of Bachelor of Engineering
(Honours.) Electrical and Electronic Engineering**

**Lee Kong Chian Faculty of Engineering and Science
Universiti Tunku Abdul Rahman**

April 2019

DECLARATION

I hereby declare that this project report is based on my original work except for citations and quotations which have been duly acknowledged. I also declare that it has not been previously and concurrently submitted for any other degree or award at UTAR or other institutions.

Signature : _____

Name : _____

ID No. : _____

Date : _____

APPROVAL FOR SUBMISSION

I certify that this project report entitled “**AIR CONDITIONAL REFRIGERANT PIPE LEAKAGE LOCATION IDENTIFICATION USING OPTICAL SENSORS**” was prepared by **JACKY KHO SENG YONG** has met the required standard for submission in partial fulfilment of the requirements for the award of Bachelor of Engineering (Honours) Electrical and Electronic Engineering at Universiti Tunku Abdul Rahman.

Approved by,

Signature : _____

Supervisor : _____

Date : _____

Signature : _____

Co-Supervisor : _____

Date : _____

The copyright of this report belongs to the author under the terms of the copyright Act 1987 as qualified by Intellectual Property Policy of Universiti Tunku Abdul Rahman. Due acknowledgement shall always be made of the use of any material contained in, or derived from, this report.

© 2019, Jacky Kho Seng Yong. All right reserved.

ACKNOWLEDGEMENT

This project would not be a success without the help of many parties. First of all, I would like to express my gratitude towards my Final Year Project (FYP) supervisor, Ts Dr Pua Chang Hong for his selfless help in this project. He taught me the basic knowledge and skills needed to conduct this experiment that was related to optical sensors which was completely new for me. Moreover, I would like to thank Dr Pua's Master student Law Zi Jian for his help in this project. He helped to give advice and solution for certain problems I faced in this project.

Next, I would like to thank UTAR for giving me this opportunity to do my project. UTAR has provided the venue and location for the setup of this project. UTAR has also funded some of the equipment used by me in this project allowing me to had the opportunity to try something new.

Besides, I would also like to thank my friends which are in university or not. Some of them helped to provide advice that I could take in performing this project. Others help to provide moral support for me so I had the confidence to complete this project.

Last but not least, I would like to dedicate my gratitude towards my parents. Without them, I would not have been able to study in university let alone the opportunity to carry out this project. They helped to ensure that finance would not be a part of a problem that I had to deal with so I could concentrate on doing well in this project.

ABSTRACT

Pipeline leakage in air conditioner has always been a problem accompanied with air conditioner. Leakage detection has therefore become a popular study to stop this problem. A much better and accurate leakage detection method is needed as high rise building and large commercial building uses centralized air conditioner system where pipelines are concealed in concrete walls making traditional leakage detection methods such as bubble soap test to be impossible. This experiment aims to mitigate refrigerant leakage through localization of leakage using optical sensors working together with machine learning (ML) algorithms. Optical sensor collects data of acoustic vibration of the pipeline system and uses a NI DAQ as interface to connect with LABVIEW. LABVIEW is used to collect the data from the optical sensors and to process the data with three ML module known as Support Vector Machine (SVM), Neural, and Logistic Regression. Three conditions are considered in this experiment which is no leakage, small leakage, and leakage. Therefore, this experiment focuses on detecting leakage through optical sensors and classification with machine learning.

TABLE OF CONTENTS

TABLE OF CONTENTS	vii
LIST OF TABLES	ix
LIST OF FIGURES	x
LIST OF SYMBOLS / ABBREVIATIONS	xi
LIST OF APPENDICES	xii

CHAPTER

1	INTRODUCTION	1
	1.1 General Introduction	1
	1.2 Importance of the Study	3
	1.3 Problem Statement	4
	1.4 Aims and Objectives	4
	1.5 Scope and Limitation of the Study	4
2	LITERATURE REVIEW	5
	2.1 Air conditioner	5
	2.2 Leakage detection	6
	2.2.1 Negative Pressure Wave	6
	2.2.2 Acoustic Detection	10
	2.2.3 Volume Mass Balance	12
	2.2.4 Optic Fibre Detection	13
	2.3 Cross-correlation	14
	2.3.1 Non-dispersive guided wave mode	15
	2.4 Summary	16
3	METHODOLOGY AND WORK PLAN	17
	3.1 Introduction	17

3.2	Experimental Setup	17
3.3	Data Analysis	21
3.4	LABVIEW	22
3.5	Summary	27
4	PREMINARY RESULTS	28
4.1	Introduction	28
4.2	Overall Results Obtained	28
4.3	Discussion	31
4.4	Summary	33
5	RECOMMENDATIONS AND CONCLUSIONS	34
5.1	Recommendations	34
5.2	Conclusion	34
	REFERENCES	35
	APPENDICES	41

LIST OF TABLES

Table 1.1: Types of leakage detection	2
Table 2.1: Component of air conditioner and their functions	5
Table 2.2: Data issues and their description	6
Table 2.3: Difference between Raman and Brillouin distributed sensing technique	13
Table 2.4: Number of leakage and their estimated leakage location	15
Table 3.1: Functions of equipment used in experiment	20
Table 3.2: Classification of leakage statuses of each sensor	26
Table 4.1: Results obtained from testing data obtained on same day with trained model	28
Table 4.2: Results obtained from testing data based on overall trained model	29
Table 4.3: Different test data deployed on different trained model dates (without small leakage)	30
Table 4.4: Different test data deployed on different trained model dates (with small leakage)	30

LIST OF FIGURES

Figure 1.1: Parts of Optical Fibre	3
Figure 2.1: Evaporation Cycle	5
Figure 2.2: Wavelength Propagation for Raman and Brillouin method	14
Figure 3.1: Block diagram of experiment	17
Figure 3.2: Practical setup of experiment	18
Figure 3.3: Experimental setup connected to Laptop	19
Figure 3.4: Initial leakage valve used	19
Figure 3.5: Flowchart of data processing	21
Figure 3.6: LABVIEW setup diagram for collection of data	22
Figure 3.7: DAQ setting	23
Figure 3.8: Configuration of wavelet denoise	24
Figure 3.9: Selecting CSV file to be trained	24
Figure 3.10: Choosing the machine learning algorithm preferred	25
Figure 3.11: Saving JSON file of trained data	25
Figure 3.12: Testing data to predict accuracy of trained data	26
Figure 4.1: Average accuracy of different machine learning algorithms against different type of deployment methods	29
Figure 4.2: 18/2/2019 SVM model deployed on 18/2/2019 test data without small leak	31
Figure 4.3: 18/2/2019 Neural model deployed on 18/2/2019 test data with small leak	31

LIST OF SYMBOLS / ABBREVIATIONS

V	Poisson's ratio of host structure material
l_{eff}	Effective length fraction in direction '1'
b_{eff}	Effective width fraction in direction '2'
d_{31}	Piezoelectric coefficient relate to normal strain in direction to a field along poling direction '3'
E_c	Young Modulus of PZT Material
l_c	Length of PZT sensor in direction '1'
b_c	Width of PZT sensor in direction '2'
C_F	Feedack capacitance of the charge mode amplifier circuit
v	Propagation velocity of negative pressure wave in pipeline
x	Distance between leak point and upstream sensor
t_1	Time when wave is detected by sensor one
t_2	Time when wave is detected sensor two
u	Velocity of natural gas in pipeline
$v(x)$	Complex propagation velocity of negative pressure wave
$u(x)$	Complex velocity of natural gas in pipeline

LIST OF APPENDICES

Appendix 1: Schematic of NPW Propagation	41
Appendix 2: MATLAB code to process LVM to CSV files	42
Appendix 3: Sample of LVM file	42
Appendix 4: Sample of training CSV file	43

CHAPTER 1

INTRODUCTION

1.1 General Introduction

Ever since air conditioner has been invented in 1902 by Willis Haviland Carrier (Willis Carrier, 2018), it has been evolving from a premium luxurious equipment into more of a necessity throughout this century. Based on Arnold (1999), majority of air conditioner users in United States (US) was “commercial comfort” air conditioning from 1920 to 1960 with the motive of attracting more customers. However, Grieser (2012) states that with the hotter summer trends and record-warm overnight temperatures becoming more frequent, air conditioning has become a must for our health and well-being. Besides, research shows that human being’s efficiency of working capacity has increased due to the presence of air conditioner (Khemani and Stonecypher, 2007). The comfort environment created by the air conditioner allows the person to have a peace mind and produce a qualitative work. Hence, the exponential growth of usage in air conditioner is unavoidable when 84% of US citizens have air conditioner installed in their house which is more than half of the population (Warner Service, 2018).

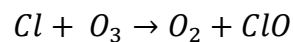
A problem that is always associated with air conditioner is refrigerant pipeline leakage. Symptoms of refrigerant leakage includes (Signs And Effects Of Refrigerant Leak In Air Conditioners, 2018):

- i) Lower cooling capacity
- ii) Air conditioner not producing cold air
- iii) Noisy air conditioner

Refrigerant leakage is normally caused by the wear and tear due to constant usage of air conditioner. Inefficient operation during the usage of air conditioner produces excess vibration that forces the refrigerant to tear a hole. Another reason is corrosion caused by presence of air and oxygen that is unpreventable which produces holes in the pipeline (What Causes Refrigerant Leaks?, 2017). Furthermore, formicary corrosion occurs when formaldehyde is present that forms formic acid in air conditioner coil and creates pin holes in the copper tube over time causing leakage (3 Common Causes of AC System Refrigerant Leaks, 2013). Goodman (2015) states that

formaldehyde originates from building products such as plywood, fibreboard, glues and adhesives.

Refrigerant contains freon which is a colourless gas that is harmful to human body and the environment. According to Carey and Cafasso (2015), excessive inhalation of freon can lead to breathing problems, organ damage and even sudden death to humans. A case happened in recent past years at a business in Hammonton, where eight people had inhalation injuries with symptoms such as tightening of chests and a burning sensation due to refrigerant leakage (Post, 2015). Furthermore, freon is recognised to be one of the main contribute to depletion of Earth's ozone layer due to the chlorine, Cl, in the refrigerant. The interaction between Cl and ozone is described using the equation below (Baum, 2017):



This equation shows the breakdown of ozone layer into oxygen and another molecule. Another impact of refrigerant on the environment is global warming. The release of CFC, HCFCs and HFCs during refrigeration leakage is part of greenhouse gases. Hence, pipeline leakage will not only cause fatality to human but also damages to the environment.

These problems have led to the case where leakage detection and monitoring is required to prevent all these hazards from occurring. One of the common traditional detection includes the bubble leak testing where soap solutions are applied over the pipeline to detect leakage. If there is any leakage at the pipelines, bubbles will be formed around it (Air/Soap Test, 2018). However, this detection works only when leakage has already occurred and does not provide any monitoring. Development of technology has produced advanced detection method used currently which are separated into software based and hardware based as shown in Table 1.1 (Penner et al., n.d.). Software based focuses on the internal parameters of the pipeline meanwhile hardware based focuses on inspection on external of the pipeline.

Table 1.1: Types of leakage detection

Software based detection	Hardware based detection
Volume balance	Acoustic emission
Transient Models	Fibre optic sensing
Pressure Analysis	Vapor Sensing Method

Basically, fibre optic sensing is performed through fibre optic sensors. Fibre optic sensors use optical fibre to detect physical quantities such as pressure and mechanical strain (AZoSensors, 2014). As shown in Figure 1.1, optical fibre is defined as a thin rod of high-quality glass (Sending information, 2018), made from three parts: Core, cladding and coating (Fidanboyly and Efendioglu, 2009). The core is the main part where all signal transmission occurs, cladding causes reflection of waves to produce a path for signal to pass through and lastly the coating is added to protect the optical fibre (Cable Basics: Fiber Optic Cable, 2018). Fibre-optic cable allows light to travel in it through the phenomenon total internal reflection. Light contains the information required to be processed or analysed and bounces through the walls until its targeted destination (Woodford, 2018). Optical fibre is used in this study as the sensor to detect pipeline leakage.

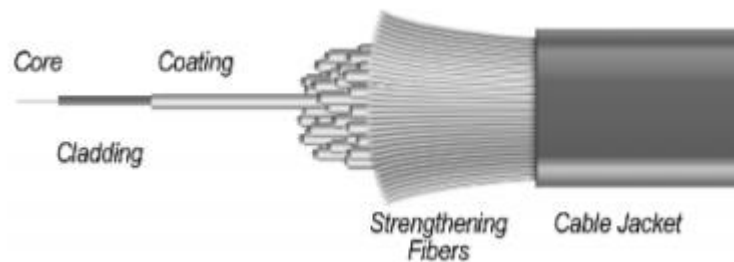


Figure 1.1: Parts of Optical Fibre

This study aims to produce a monitoring system that detects leakage and position of leakage using optical sensor that detects acoustic vibration through utilising LABVIEW's machine learning algorithms.

1.2 Importance of the Study

Main focus of this project is to mitigate refrigerant leakage and to locate the position of leakage in air conditioners using optical sensors through utilisation of LABVIEW. LABVIEW provide simple graphical user interface (GUI) setup with the capability of performing real-time monitoring and detection through data collection, processing, and analysis. This study exploits the capability of optical sensor to be applicable in leakage detection and monitoring field.

1.3 Problem Statement

Pipeline leakage being not a nuisance unnoticed, but it becomes detectable rapidly to be solved.

Exponential evolution of air conditioner usage in shopping complexes or large buildings has led to complicated pipeline system. This complicated pipeline system has caused the detection of pipeline leakage to become more difficult. Furthermore, the refrigerant pipeline is normally concealed in the concrete wall or ceiling partition which causes the conventional detection method become rather impossible. Pipeline leakage can cause the air conditioner to be less cold in the shopping complexes and cause losses for their owners. To overcome this, pipeline leakage detection is performed through optical sensors in compliance with LABVIEW for constant monitoring of pipeline system. Machine learning is deployed where classifications for various status of leakages are performed.

1.4 Aims and Objectives

This study has three main objectives to be achieved. First, this study strives to detect leakage and position of leakage in pipeline using optic sensors. The next objective is to monitor pipeline system of air conditioner. Lastly, it is to optimize the detection and reduce false alarm.

1.5 Scope and Limitation of the Study

This study uses only a small pipeline system as compared to complex pipeline system. Besides, only one brand and specific type of air conditioner is used, which is a wall mounted Daikin. Furthermore, Universal Serial Bus (USB) is required for monitoring which means this is not suited for long distance monitoring.

CHAPTER 2

LITERATURE REVIEW

2.1 Air conditioner

Air conditioner as its name implies is a machine that conditions our air which means to control the temperature and humidity of the surrounding to suit our needs. Components of air conditioner can be separated into the hot side located outside the home which includes the condenser, compressor and fan whereas the cool side located inside the home has the evaporator and another fan as shown in Figure 2.1 (Components of an air conditioning system, 2013). The functions of the following components are shown in Table 2.1 below (Brain, Bryant and Elliot, 2018):

Table 2.1: Component of air conditioner and their functions

Components	Functions
Evaporator coil	Holds the cold refrigerant and evaporate to absorb heat from surrounding.
Condenser coil	Warmed refrigerant from evaporator coil is passed here to be condensed and release the excess heat.
Expansion valve	Controls the flow of refrigerant flow.
Compressor	An electrical pump that utilize high pressure to compress the refrigerant gas into liquid.
Fan	Pushes the air from evaporator coil and condenser coil.
Refrigerant	A chemical that transforms from liquid to gas easily (The Purpose of Refrigerant in Air Conditioning Systems, 2018).

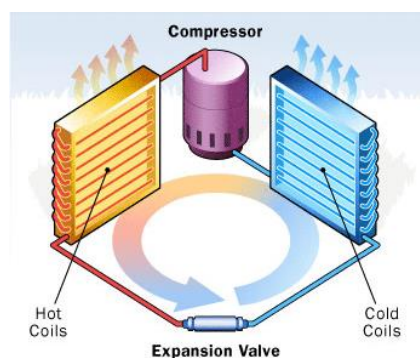


Figure 2.1: Evaporation Cycle

2.2 Leakage detection

Refrigerant leakage frequently occurs on the evaporator coil (Evaporator Coil, 2018). Evolution of the modern world has led to the exponential growth in usage of pipeline, whether in transportation, industrial and residential. All these pipelines regardless of their usage categories eventually faces one similar problem which is pipeline leakage. Pipeline leakage is an unwanted effect that not only affects us human and also the environment. However, removing this issue is an impossible task and has resulted in researches regarding the detection and localization of leakage being a trending topic. Techniques of leakage detection can be separated into hardware and software based on Table 1. Then, according to Walk (2010), leakage detection system (LDS) can be separated into two categories, internal and external detection system. Internal LDS focuses on usage of mathematical algorithm that integrates to form a control system using SCADA. External LDS use hardware such as optic fibre and thermostats to collect data work in parallel with the internal LDS. Leak detection system differs from leakage detection as it consists of monitoring and collection of data from the pipeline.

2.2.1 Negative Pressure Wave

Negative pressure wave (NPW) operates using the conservation of energy principle, gas is released to the surrounding whenever a leak occurs resulting in a pressure drop in the pipeline. This pressure drop generates a wave to both ends of the pipeline known as the NPW (Negative Pressure Wave Description, 2018). NPW commonly works together with pressure transducer to collect data.

2.2.1.1 Challenges and Algorithms

Based on Table 2.2, NPW have the following data quality issues which is missing data, data duplication and noise.

Table 2.2: Data issues and their description

Data Issue	Description
Missing data	Missing of data during transmission due to clock synchronization
Data duplication	Few values duplicated during transmission due to clock synchronization
Noise	Two sources: i) Spike noise – Comes from data collection

	ii) Stationary noise – Comes from circuit or pipe hydraulics
--	--------------------------------------------------------------

The autoregressive-moving average model (ARMA) filtering method is used for this case where it shows that filtering affects the accuracy of the position. A higher signal to noise ratio (SNR) would also affect the accuracy of the detection of leakage position. Hence, filtering method needs to consider a balance in between the effectiveness of the SNR and accuracy of leakage detection.

To determine leakage from the data collected, threshold method is used where values exceeding the threshold set would be a possible leakage point. However, this method is not accurate as different pipeline has different threshold value and is easily affected by external factors. Statistical Process Control (SPC) which is another method is used where large quantity of samples is required to overcome this problem.

Few ideas were proposed to reduce the false alarm rate that includes using other leak detection method (such as optic fibre), flow meter to determine the downstream or upstream operation condition change, and pattern matching algorithm. The author uses multiple sensor pairing method to reduce the false alarm rate. Accuracy of this detection is affected by the assumption of constant NPW speed and time synchronization of the device. In practical case, the NPW speed is around 0.9 – 1.2 km/s. In most of the cases, NPW speed is always assumed constant due to practical limitation and the cost (Tian et al., 2012).

2.2.1.2 NPW with PZT sensors

Lead zirconate titanate which is commonly known as PZT is used as a sensor in this research to detect pipeline leakage. PZT is commonly used in medical imaging processes (Piezoelectric Effect, 2018). PZT material can either generate electric charge upon mechanical strain or undergo deformation when there is an electric field applied upon it (What is PZT?, 2018).

PZT sensor is used to detect the variation of hoop strain when leakage occurs in this research. Variation of hoop strain occurs when NPW is generated as the pressure drop causes a contraction of pipe wall. Strain detected by the PZT causes it to generate an output voltage based on the equation below:

$$V_o = (1 - V)(l_{eff}b_{eff}) \frac{d_{31}E_c l_c b_c}{C_F} \epsilon_{11} - (1)$$

Based on the equation above, the l_c affects the sensitivity of the sensor towards the hoop strain whereas the b_c controls the signal strength that is the response duration of the signal. Therefore, it is recommendable for the l_c to be much greater than b_c . When there is no NPW, the output voltage would always be in the condition of 0 V as there is no deformation or mechanical strain detected.

Experimental setup of this research was done with flat patched PZT sensors mounted directly on the pipeline. Results obtained indicates that the maximum error was 2% while using a 55 meter pipeline and repeatable location of 4% variance for 5 leakage points. Superposition of incident and reflected NPW has resulted in the delay in the result obtained when the sensor is too close to the end of the pipelines. This effect has caused the leakage closer to the end of the pipelines have the largest error than other leakages.

Improvements that could be performed to improve the experimental result includes using l_c that is so much higher than b_c . Besides, the PZT sensors could be made to bend and wrap around the pipeline. PZT sensors are also not that practical to be installed along long distance of pipelines (Zhu et al., 2017).

2.2.1.3 Using FBG Based Strain Sensor

Fiber Bragg grating (FBG) sensor offers more advantageous benefits as compared to pressure sensor. Pressure sensor has larger signal attenuation and interference as their sensors are only attached at ends of pipeline system. As the pipeline system becomes longer, it is unavoidable that the accuracy of the detection will decrease together while the rate of false alarm will be increased. As compared to pressure sensor, FBG is immune to electromagnetic interference, responds very quickly to temperature change, do not corrode, and can measure up to 30,000 micro strain (What are the Specific Advantages of FBG Sensors?, 2018).

FBG sensor is used as a strain sensor and wrapped around the pipeline to measure the change in the hoop strain of the pipeline when there is a leakage. Appendix A shows the experimental setup of this experiment. Common leak location formula that assumes velocity of NPW is always assumed constant is shown below:

$$t_1 = \frac{x}{(v - u)}$$

$$t_2 = \frac{(L - x)}{(v + u)}$$

$$\Delta t = t_1 - t_2 - (2)$$

$$x = \frac{1}{2v} [L(v - u) + \Delta t(v^2 - u^2)] - (3)$$

where t_1 and t_2 represents the time signal is received by each signal representatively, x is the distance between the leak point and its upstream sensor, v which represents speed of NPW, and u is the velocity of natural gas.

$$t_1 = \int_0^x \frac{1}{v(x) - u(x)} dx - (4)$$

$$t_2 = \int_x^L \frac{1}{v(x) + u(x)} dx - (5)$$

Equation 2 is modified into Equation (4) and (5) where it has become a continuous function where Compound Simpson formula is used to calculate this integration above and obtain the time difference. Later on, the Dichotomy Searching is used to locate the leaking point. Lastly, wavelet transform is applied to find the sharp transition of pressure drop as it can easily scale up the signal to find the sharp transition of pressure drop. Results obtained shows that as the scale increases for wavelet transform, the fake singularities obtained becomes less frequent and the real singularities become more obvious. Final results of this experiment prove that there was only a relative error of 4.8%, considering the fact that the pipeline was very short which means the leakage detected is near to its actual leakage (Hou et al., 2013).

Another research where an array of FBG-based pressure sensors are used to detect the bending of the beam to monitor the wavelength shifts between two FBGs in opposite direction. This helps to reduce the cross-sensitivity of the FBG towards temperature variation. As the leakage is closer to the sensor, leakage would be detected much faster. NPW propagation velocity is calculated using a new formula as the actual propagation velocity is never constant. The new formula uses the distance of a set of sensors from leakage point and the time difference in receiving the signal. A new technique to reduce false alarm is proposed where the output of another sensor is considered. Leakage is determined by using sensors placed in adjacent and the time difference between these sensors determines whether there is an intense noise effect. From the experiment, traditional NPW shows a trend of increasing relative error when there is a decrease in the pressure. However, the Novel NPW-based method does not show this significance and has a lower relative error. For instance, during the leak

position of 7.8 m, Novel NPW-based method has a relative error of 0.10% whereas the tradition NPW-based method has a 0.49% relative error (Wang et al., 2017).

2.2.2 Acoustic Detection

Acoustic detection in pipeline leakage field is performed where high pressure difference between the internal and external of the pipeline generates an acoustic vibration.

2.2.2.1 Using Wavelet Packet Transformation and FSVM

Intensity of acoustic vibration is affected by the leakage diameter, which the leakage diameter increases with the increase in intensity of the acoustic vibration. Another trend that is observed is the decrease in intensity of acoustic signal when the propagation distance becomes further as diffusion occurs. Advantages of using acoustic detection is the short delay time and physical information is carried. Wavelet Packet Transform (WPT) is applied to produce a higher resolution and increased accuracy of the leakage detection as it helps to denoise the signal obtained. Then, Support Vector Machine (SVM) is applied to analyse the filtered signal from WPT to predict the location of leakage. Through comparison with other SVM method, Fuzzy Kernel Function (FSVM) is concluded to be the best with an accuracy of 99%. Position error obtained is always less than 1% which means this method is effective in detecting leakage. In actual field practice at Donglin gas pipeline, the positioning error varied from +100m to +400m with an overall length of 156 km. This means that the error is considered rather small, taking the overall length into account. Response time of the detection is also very fast from 1 – 2 minutes only. Besides leakage quantity is also discovered to be from 0.9% to 1.75% (Xu, Zhang and Liang, 2013).

2.2.2.2 LMD envelope spectrum entropy and SVM to detect leakage aperture

Acoustic vibration that occurs during leakage is detected to determine the gap of the leakage size. This study uses the pressure sensor to collect leakage signals and decomposes it into smaller several product function (PF) components using local mean decomposition (LMD). Kurtosis is then applied where the first three PF components obtained has the highest sum over 90%. This results in the selection of the three PF component to be the main component. Kurtosis is chosen as it is used to narrate the

effective sharpness of a waveform resulting in collection of signals with most leakage data. Verification of the accuracy of these PF's were conducted through the Pearson correlation where the correlation coefficient for the first three PF components were proven to be highest. Pearson's correlation helps to prove that the data under Kurtosis is related to its original signal. Then, these three PF is reconstructed using wavelet packet decomposition based on its energy distribution characteristics. Results show that 90% of the energy is concentrated on the first two PF. After that, this reconstructed PF undergoes Hilbert transformation to produce an envelope spectrum and its normalized entropy. Lastly, SVM is applied to calculate the gap of its leakage size. The test shows that the accuracy of detection ranges around from 79% to 89% for small leak sizes of 2 – 5 mm.

Through this experiment, it is observed that the envelope spectrum entropy is affected by the internal pressure of the pipeline and distance between the leakage and sensor. Another scenario noticeable in this experiment is the reduction in accuracy of leakage detection when the distance between the sensor and leakage increases (Wang, Gao and Liu, 2016).

2.2.2.3 Experimental study on denoising

Comparing between median filtering, Wiener filtering, wavelet filtering, band-pass filtering by FIR and IIR, wavelet filtering method is chosen for Gaussian white noise as it has the highest signal to noise ratio (SNR) as well as the root mean square error (RMSE) and amplitude loss of pressure drop (ALPD) lowest. If signal obtained is within same frequency band with the noise, the blind source separation method is suggested. Fast independent component analysis (FastICA) is used in this method to filter noise for same frequency band case. However, this method poses the threat of amplitude loss between leakage signal and the post signal. This method is not considered as the best filtering method as it requires dynamic pressure sensors that costs heavily but it will be used in this experiment. FastICA is affected by the number of sensors used in the experiment where as the number of sensors increase, more source signals are obtained resulting in the increased effectiveness of this method. Leak detection is then performed where the time differences were calculated using the cross-correlation algorithm.

Methods above were used in a pipeline with an inner diameter of 42 mm and the largest location error obtained was 0.874% under 0.4 MPa for gas (Liu et al., 2017).

2.2.2.4 VMD and CTFS with piezoelectric vibration sensor

Common acoustic emission detection technique utilises cross-correlation which assumes propagation velocity of the acoustic wave is constant that has a poor accuracy due to dispersive nature of wave along pipe and signals collected are non-stationary. Variational mode decomposition (VMD) is a useful non-stationary signal processing method where centre frequencies and bandwidth of mode components are determined through the decomposition process. Main advantage of this method is its ability to eliminate mode mixing and has strong noise immunity. Certain mode components produced from VMD exists as sensitive components that are highly connected to the leakage signal while some others just interferences. Due to this reason, mutual information is applied between original signal and decomposed signal to get only the sensitive components while ignoring the interferences. Cross-time-frequency spectrum (CTFS) is proposed as a method to process non-stationary signal. CTFS works based on cross-correlation where the function of delay and corresponding frequency is joint together to describe spectral components of signals during different time delays. Different kernel function in CTFS has different results, research is carried on the Wigner-Ville Distribution (WVD), Polynomial Wigner-Ville Distribution (PWVD) and smoothed pseudo Wigner-Ville Distribution (SPWVD) to process the signal from VMD. SPWVD shows the best result for delay and frequency information whereas WVD has the poor results due to serious cross-term interference.

Based on the data collected, empirical mode decomposition (EMD) method has an error around three times higher than the VMD method due to its high cross-term interference. VMD has an error of around 0.34 – 1.29 m only whereas EMD has an error from 1.17 – 2.95 m. Another group of data processed shows that the average relative error for EMD is 8.34 due to mode mixing while VMD only has an average of 2.78 as it decomposes non-stationary signal and solves mode mixing (Xiao et al., 2018).

2.2.3 Volume Mass Balance

One of the common methods for software leak detection where the mass and volume flow into and out of the system is required to be in equilibrium. Leakage is detected

when this equilibrium is broken which means that the mass exiting is more than the estimated mass entering the pipeline. Normally, this method works with a Supervisory Control and Data Acquisition (SCADA) system for monitoring and efficient control of the system.

2.2.3.1 Online Simulation Method

Experiment conducted under no steady state as it operates on a demand basis. This experiment uses a modified volume mass balance to predict leakage. An assumption where potential leakage occurs for every mismatch in mass balance is made. First, pressure balance and flowrate in pipeline is collected by SCADA. Then, potential leakage is compared with its threshold to determine whether leakage occurs or not. When the potential leakage is higher than its threshold, it is deduced that leakage occurs.

Some problems faced during this research includes the unreliable data acquisition, unexpected low resolution of pressure sensor and uncontrolled fluctuation. Results obtained in this research shows that the average location error is around 4 – 20% from maximum load to minimum load. However, under extreme transient condition the average location error is around 6% (Fukushima et al., 2000).

2.2.4 Optic Fibre Detection

One of the famous detection methods for optic fibre is the temperature-based leak detection where it detects a change in the temperate of the pipeline during leakage. Leakage of gas results in the Joule-Thompson effect where temperature of the surrounding would be decreased due to expansion of gas (Omnisens, 2001). Two famous distributed sensing technique known as the Raman and Brillouin technique where their differences are shown in Table 2.3 below.

Table 2.3: Difference between Raman and Brillouin distributed sensing technique

Raman	Brillouin
Measures temperature profile only	Measures temperature or strain
Generated by thermally influenced molecular vibrations	Combination formed from interaction between propagating optical signal and thermally acoustic waves
Depends on intensity	Depends on frequency

Applicable with multimode fibres	Applicable with single mode optical fibres
High sensitivity only for short distance	Higher accuracy and sensitivity for longer distance

In addition, Raman scattered light consists of two frequency shifted components known as the Stokes and Anti-Stokes component where the former has its amplitude related to temperature while the other does not. Therefore, Raman method requires filtering to remove this Anti-Stokes that is unnecessary signal (Mishra, Soni and Delhi, 2011). Figure 2.2 below also shows the difference between the wavelength propagation for the Brillouin and Raman method.

Based on the results from Nikles et al. (2004), leakage that occurred in the pipeline resulted in a local temperature increase of 8 °C by using DiTeSt analyser that operates based on Brillouin scattering.

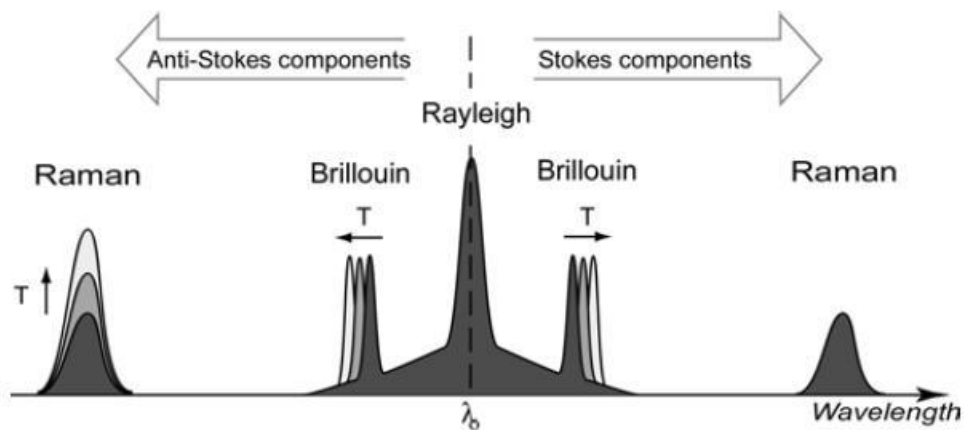


Figure 2.2: Wavelength Propagation for Raman and Brillouin method

2.3 Cross-correlation

According to Bourke (1996), cross-correlation can be defined as a statistical measurement degree of similarity between two functions or series. Cross-correlation formula is shown below (Cross-Correlation, 2018):

$$f(t)g(t) = \int_{-\infty}^{\infty} f(\tau)g(t - \tau)d\tau$$

where $f(t)$ and $g(t)$ are continuous function.

Cross-correlation determines the time delay between acoustic vibrations produced by leakages(Gao et al., 2017). This time delay is then used to determine its position of leakage by utilizing the propagation speed of the acoustic wave.

Cross-correlation can be used to detect multiple leakage signals where it is very effective during a high SNR. Two sensors are placed at both ends of the pipeline and the results collected for multiple leakage signals are collected as shown in Table 2.4. Exact location of leakage is done at 20 m, 40 m, 60 m and 90 m which is very close to the leakage positions obtained from cross-correlation method (Elandalibe, Jbari and Bourouhou, 2016).

Table 2.4: Number of leakage and their estimated leakage location

	First Leakage Estimated (m)	Second Leakage Estimated (m)	Third Leakage Estimated (m)	Fourth Leakage Estimated (m)
One Leakage	19.985	-	-	-
Two Leakage	19.985	39.985	-	-
Three Leakage	19.985	39.985	60.005	-
Four Leakage	19.985	39.985	60.005	90.02

2.3.1 Non-dispersive guided wave mode

An improvement that could be done to traditional cross-correlation is explained below. Basically, single mode waveform is extracted from cross spectrum in leakage using weighing window with parameters related to its wavenumber of the consequent mode. Then, this single mode waveform undergoes Inverse Fourier Transform to get its single-mode cross-correlation for approximating a more accurate time delay.

Comparison between results for traditional cross-correlation method and single-mode cross-correlation method is done where the first one has a relative error of 2 m meanwhile the latter one only has a relative error of 0.74 m which is less than 1 m. Besides, average relative location error obtained from single- mode cross-correlation method is around 1.38% meanwhile traditional cross-correlation method exceeds it by more than 7% ranging mostly from 10% to 19.31% (Fukushima et al., 2000).

2.4 Summary

Section 2.1 of this section talks about air-conditioner and its functions. Besides, highlight of our study is also known here which is the location where pipeline leakage occurs. Section 2.2 focuses on the recent trends of leakage detection over the recent years. Section 2.3 explains about cross-correlation and recent researches on it.

CHAPTER 3

METHODOLOGY AND WORK PLAN

3.1 Introduction

This experiment uses a National Instrument (NI) Data Acquisition (DAQ) 9234 to obtain data from two Single Mode Fiber (SMF) optical sensor mounted on two sides of the pipeline. DAQ is used to measure electrical parameters such as voltage with a computer (What Is Data Acquisition?, 2018). DAQ acts as an interface that connects the sensor with the computer for data collection. Data collected are then processed and analysed through LABVIEW to perform leakage detection.

3.2 Experimental Setup

A pair of optical sensors are attached on a pipeline for a single 1.5 horsepower air-conditioner. DAQ is connected to the optical sensors and a laptop for data collection. LABVIEW is used to monitor and record the voltage data. Leakage is produced manually through opening of valves at the pipeline to see the difference in the data collected. A simplified block diagram of the experimental setup is shown below in Figure 3.1.

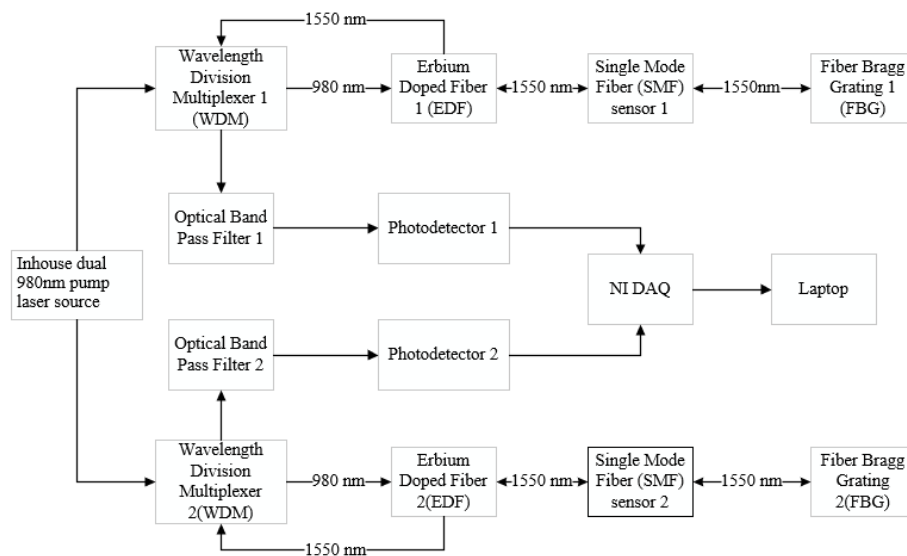


Figure 3.1: Block diagram of experiment

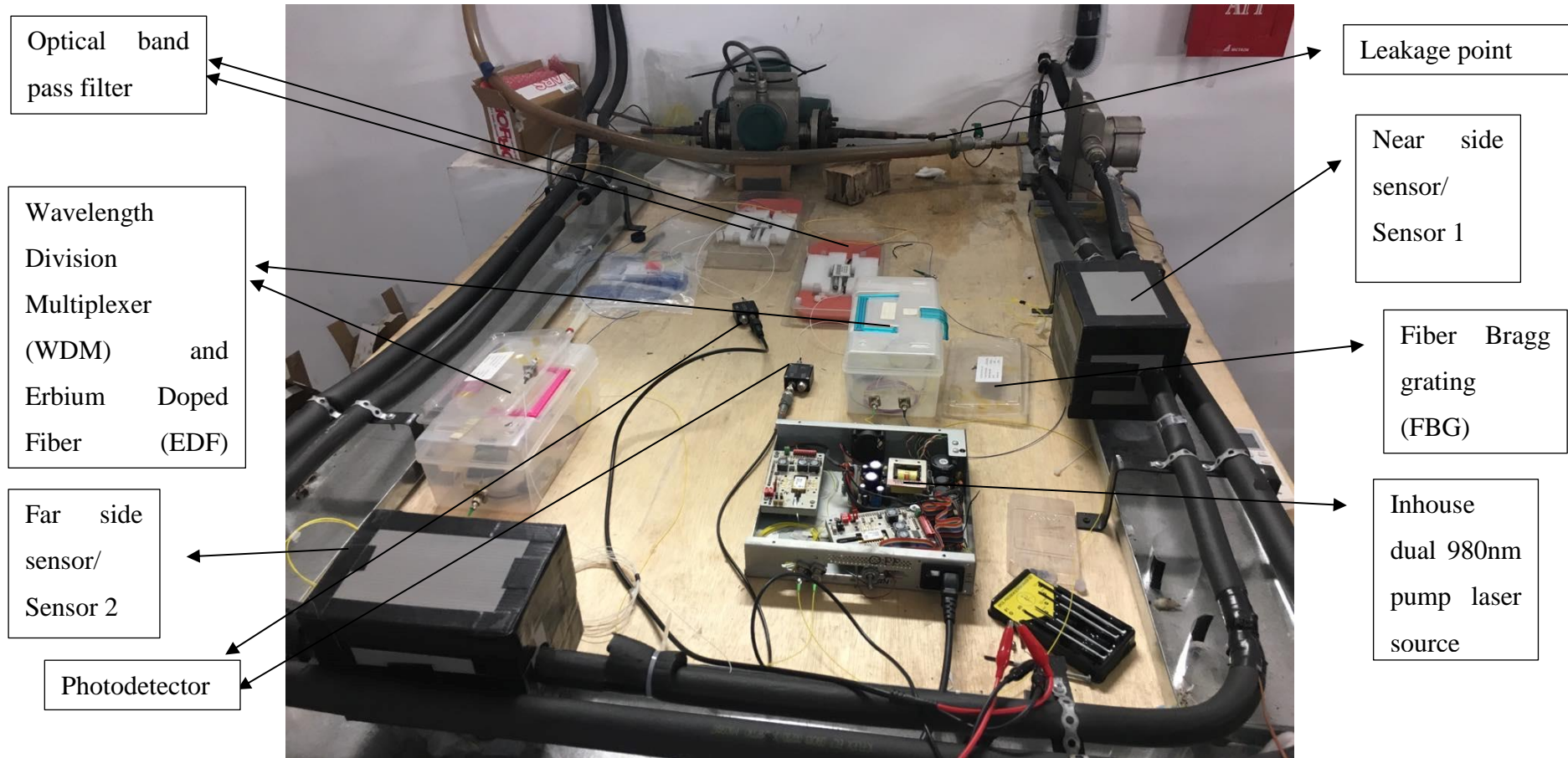


Figure 3.2: Practical setup of experiment

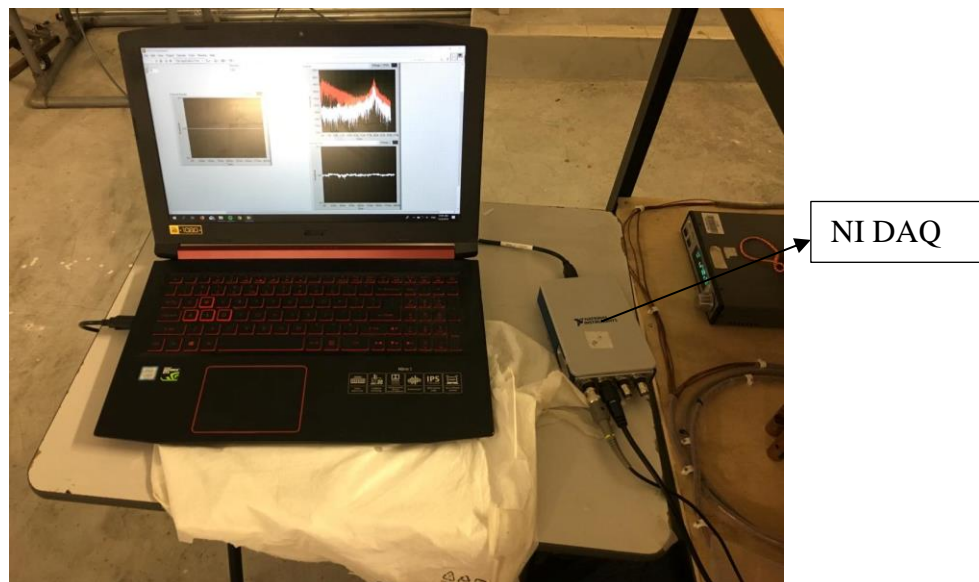


Figure 3.3: Experimental setup connected to Laptop

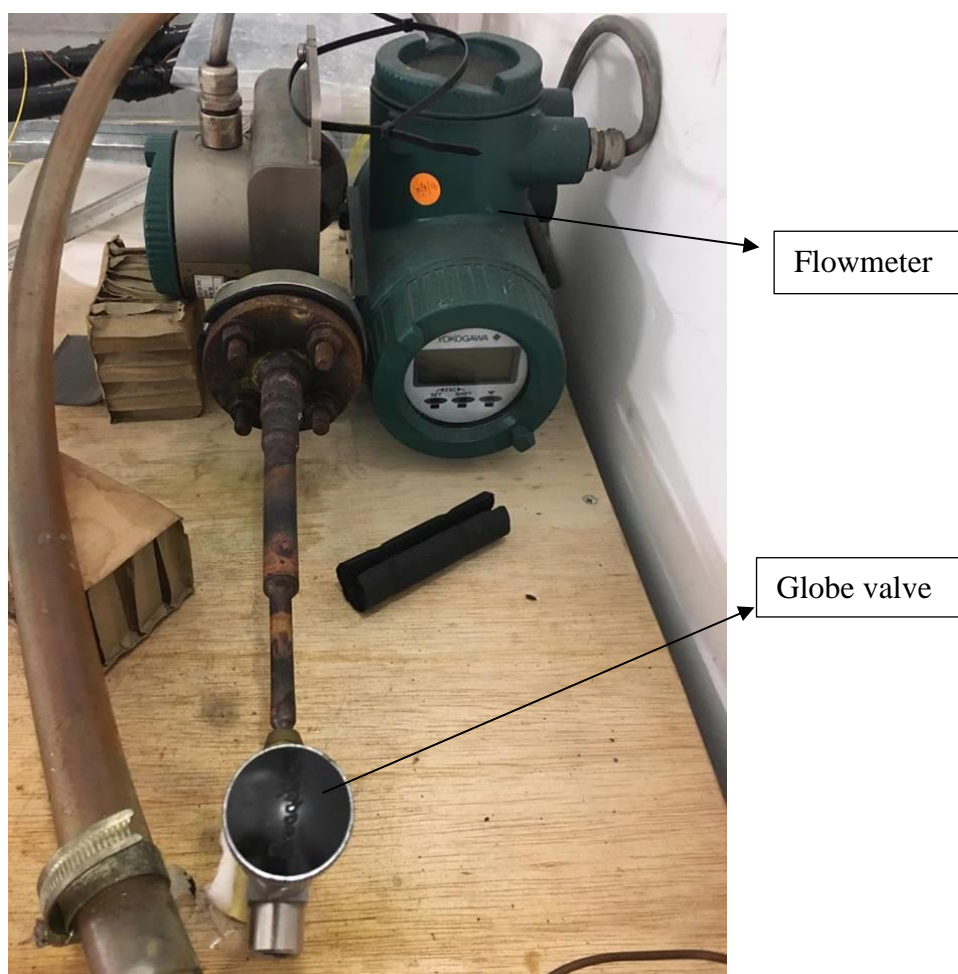


Figure 3.4: Initial leakage valve used

Figure 3.2 and 3.3 shows the practical setup of the experiment. Functions of the equipment used are shown in the Table 3.1.

Table 3.1: Functions of equipment used in experiment

Equipment	Function
Inhouse dual 980 nm pump laser source	Generates two laser sources of 980 nm.
Wavelength Division Multiplexer (WDM)	Multiplexes multiple optical signal with different wavelength into one optical fiber (THE BASICS OF WAVELENGTH DIVISION MULTIPLEXING, WDM, 2019)
Erbium Doped Fiber (EDF)	Reduces loss of optical fiber and multiply optical signals simultaneously working together with the WDM (Erbium-Doped Fiber Amplifier (EDFA), 2019)
Single Mode Fiber (SMF) Sensor	To detect the changes in acoustic vibration during leakage and no leakage condition.
Fiber Bragg Grating (FBG)	It helps to reflect specified wavelength in its narrow spectral width making it a type of narrow band filter (What is a Fiber Bragg Grating?, 2019).
Optical Band Pass Filter	Attenuate the noises produced from the 1550nm optical signal before fed into the photodetector.
Photodetector	Changes light photons or optical signals into electrical signals (PIN PHOTODETECTOR CHARACTERISTICS FOR OPTICAL FIBER COMMUNICATION, 2019).
NI DAQ	Allows the monitoring and collecting of optical sensor data through LABVIEW.

Figure 3.4 shows the initial valve used to produce leakage and a flowmeter to record the flowrate of the leakage. This needle valve was later replaced into a ball valve as shown in Figure 3.2.

3.3 Data Analysis

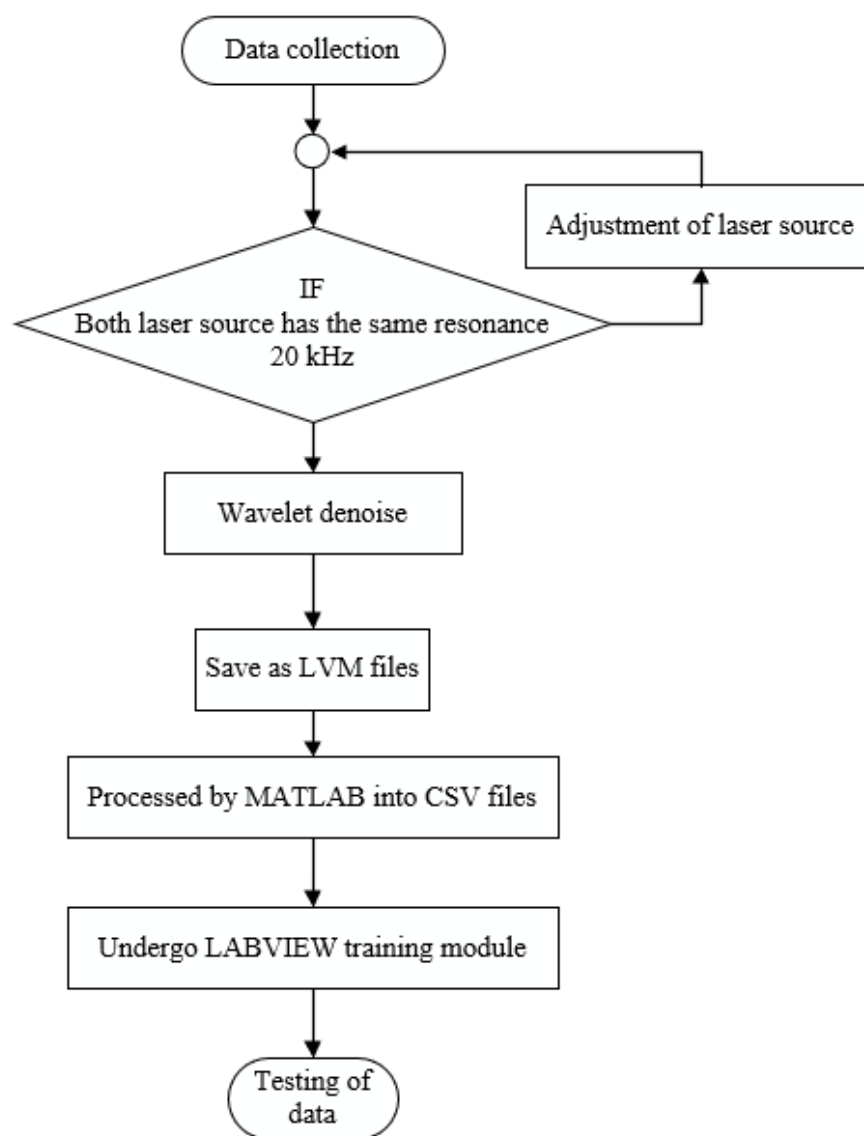


Figure 3.5: Flowchart of data processing

Figure 3.5 shows a simplified process done in this experiment to predict leakage. First, data is collected by the optical sensor and fed into LABVIEW through DAQ. Before processing any of the data, both the laser source is adjusted to have the same resonance of 20 kHz to prevent any difference in their Power Spectral Density (PSD). After the laser source has the same resonance, the data undergo wavelet denoise to remove background noises. Then, they are saved as LVM files to be later processed on by MATLAB using the code in Appendix 2. Processed files from MATLAB undergo

training in a LABVIEW module. Lastly, these trained data are used to predict new test files for leakage.

3.4 LABVIEW

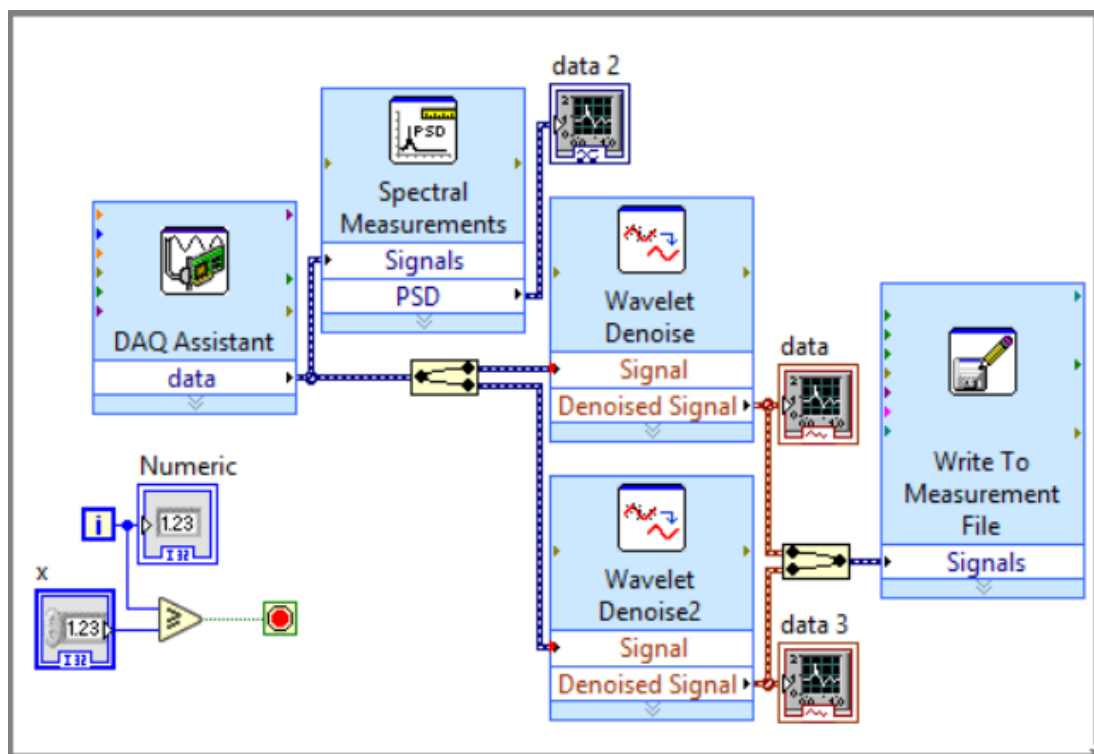


Figure 3.6: LABVIEW setup diagram for collection of data

Data collection and processing of this experiment was done using Figure 3.6 setup diagram. The DAQ assistant collects the data from the optical sensor and feeds it into the Spectral Measurement signal first to ensure that both the optical sensors have a 20kHz resonance frequency. Figure 3.7 shows the setting of DAQ used in this experiment where a sampling rate of 51.2 kHz were used. A timer of 155 equivalent to 30 seconds was set for the collection of data. Then, the signals were split into two where each of them represents a sensor and undergoes wavelet denoise to cut off unnecessary background noises in the surrounding. The settings used for the wavelet denoise was a DWT type transform with a db02 wavelet with a level of 2 as shown in Figure 3.8. The level and wavelet were set at a low level to prevent the original signal to be cleaned till it loses its characteristics. The signals are then fed into the “Write To Measurement File” to be written into LVM files. A sample of LVM files is shown in Appendix 3. These LVM files will be processed later on by MATLAB into comma-separated values (CSV) files. MATLAB processes the data from the LVM files into

kurtosis, skewness, root mean square (RMS), variance, standard deviation, mean and also their Fourier Fast Transform (FFT) as shown in Appendix 4. Later on, these CSV files are compiled and classified by the machine learning in LABVIEW. Figure 3.9 till 3.11 displays the configuration of how to train the data. As shown in Figure 3.10, three machine learning (ML) algorithms were used in this experiment which were Support Vector Machine (SVM), Neural and Logistic Regression. Trained model file would be saved in a JSON file based on Figure 3.11. Figure 3.12 shows the deployment module that will predict whether there is a leakage or not. In this experiment, small leakage is considered to be around 0.1-0.5 kg/hr flowrate meanwhile normal leakage is considered to be around 7-8 kg/hr flowrate.

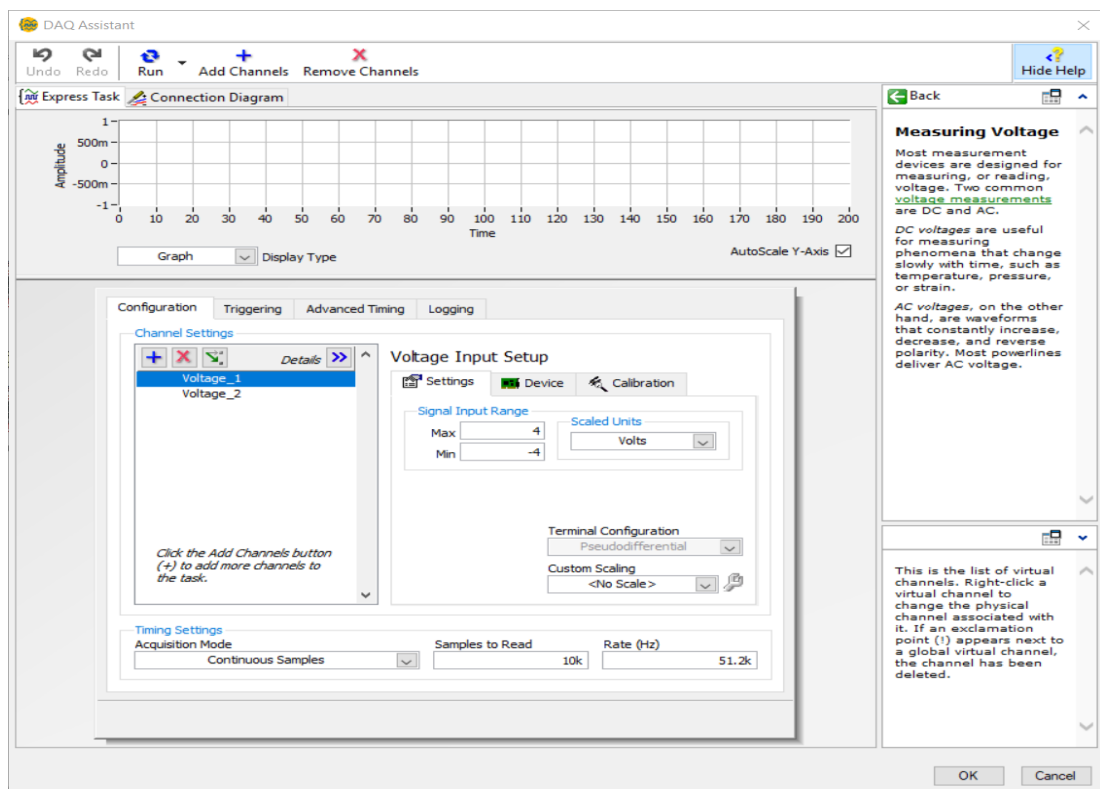


Figure 3.7: DAQ setting

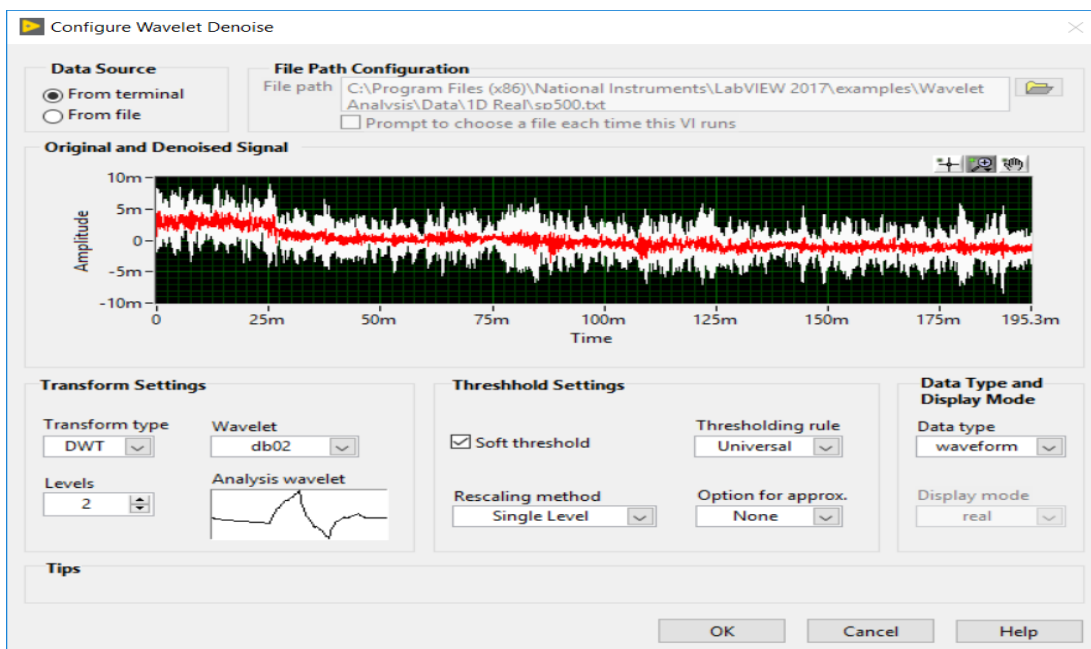


Figure 3.8: Configuration of wavelet denoise

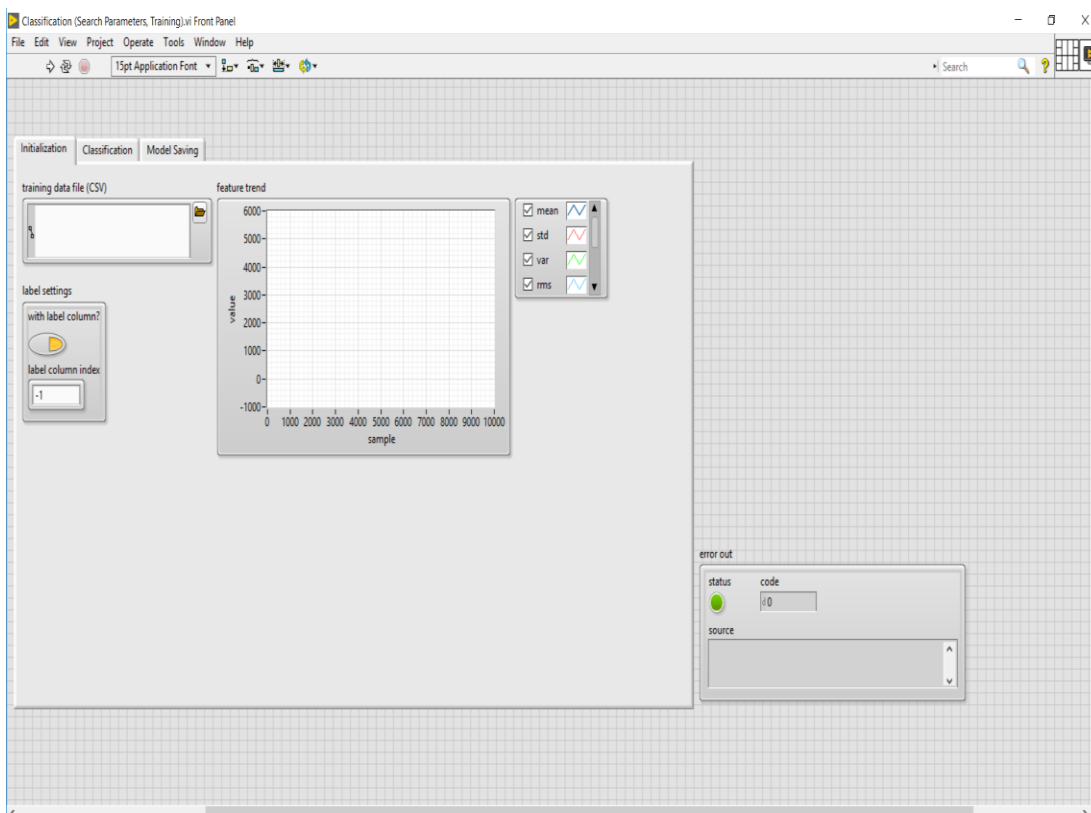


Figure 3.9: Selecting CSV file to be trained

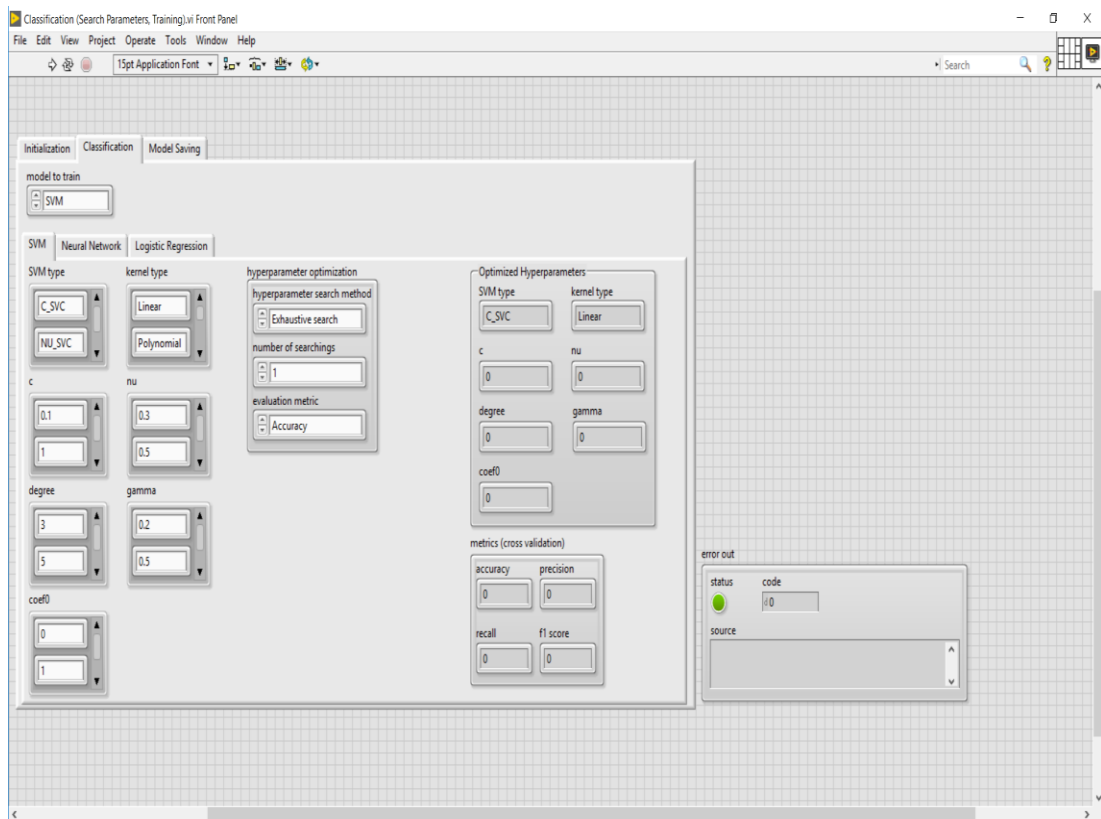


Figure 3.10: Choosing the machine learning algorithm preferred

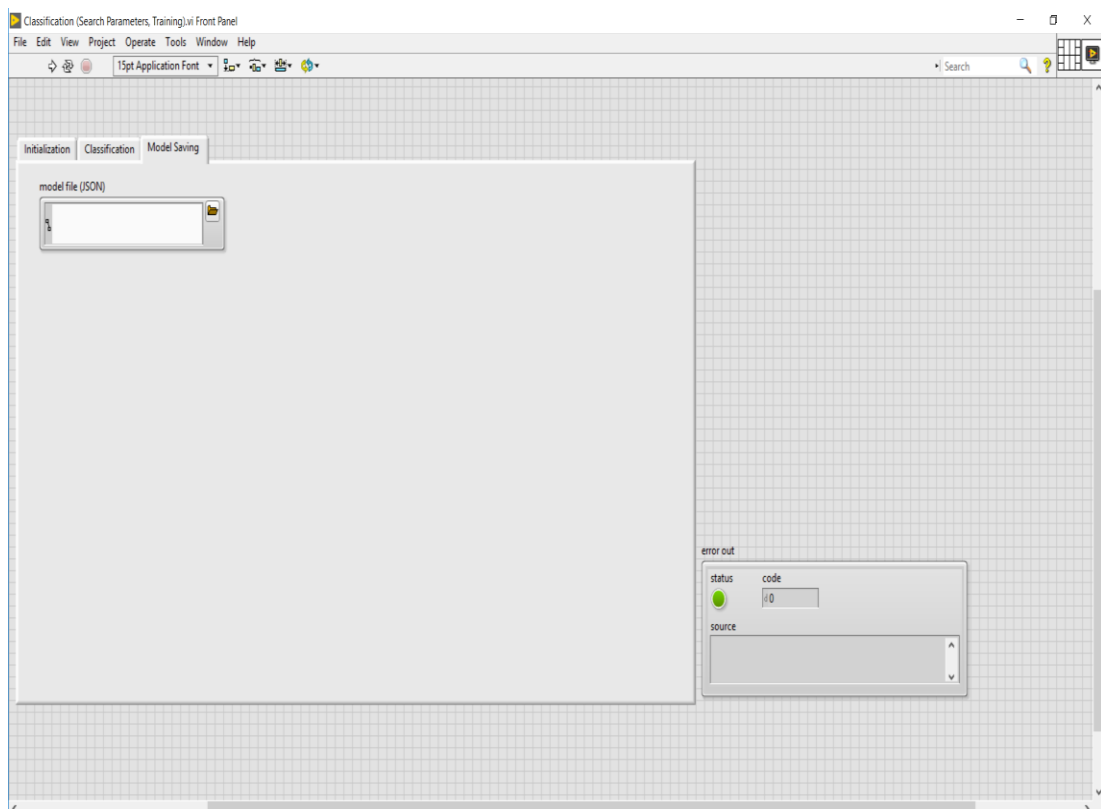


Figure 3.11: Saving JSON file of trained data

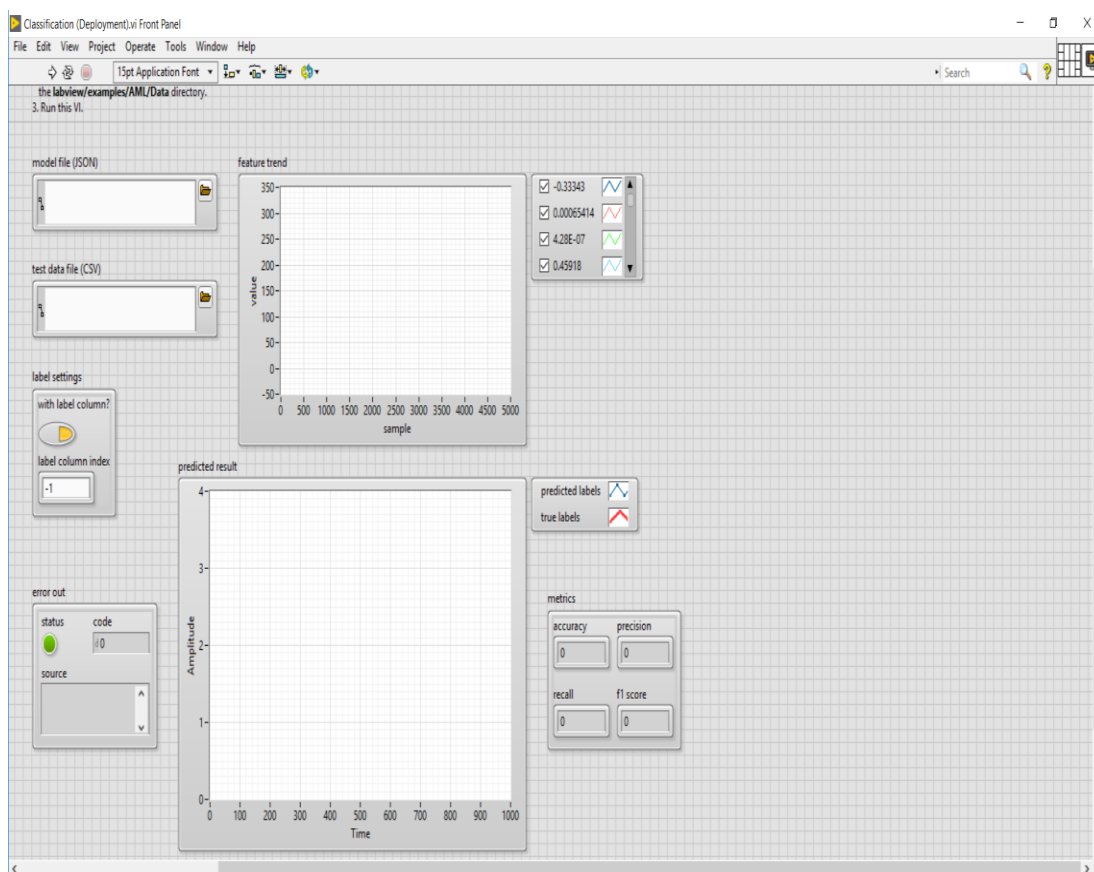


Figure 3.12: Testing data to predict accuracy of trained data

Training models are classified into 6 categories as shown in the Table 3.2 below where Sensor 1 is classified in terms of even numbers while Sensor 2 is classified in terms of odd numbers. Three types of condition named as no leakage, small leakage and leakage are considered in this experiment.

Table 3.2: Classification of leakage statuses of each sensor

Categories	Classification
Sensor 1: No leakage	0
Sensor 2: No leakage	1
Sensor 1: Small leakage	2
Sensor 2: Small leakage	3
Sensor 1: Leakage	4
Sensor 2: Leakage	5

3.5 Summary

The methodology proposed uses DAQ to connect between optical sensors and a laptop for monitoring of the pipeline system. Signal processing such as wavelet denoise is performed to improve the accuracy of the result obtained. Leakage detection is performed through machine learning algorithms to predict occurrence of leakage or not.

CHAPTER 4

PREMINARY RESULTS

4.1 Introduction

Three ML algorithms were used to compare the accuracy of these ML algorithms which were SVM, Neural, and Logistic Regression. Results obtained in this section can be separated into including small leakage and not including small leakage into the ML algorithm.

4.2 Overall Results Obtained

Results obtained in this project can be separated into four categories as shown in the tables below. First, results obtained by testing data with trained data where both are obtained on same day as shown in Table 4.1. Next, as shown in Table 4.2 where data from 18/2/2019, 20/2/2019 and 12/3/2019 are trained together into a model and separate days are tested on this trained model. Table 4.3 depicts various dates of test data deployed on different dates of trained model that does not include small leakage. Lastly, Table 4.4 shows various dates of test data deployed on different dates of trained model that includes small leakage into the machine learning. Italic word data in Table 4.3 and 4.4 represents the same results as shown in Table 4.1 where the test data date used is same with its trained data.

Table 4.1: Results obtained from testing data obtained on same day with trained model

Trained Date	ML Algorithm					
	SVM	Neural	Log	SVM	Neural	Log
	without small leak			with small leak		
18/2/2019	90.53	80.096	66.613	62.246	66.845	58.503
20/2/2019	89.263	85.897	74.039	51.403	51.403	46.752
12/3/2019	79.487	57.265	76.282	52.436	47.051	27.564
Average	86.427	74.42	72.311	55.362	55.1	44.273

Table 4.2: Results obtained from testing data based on overall trained model

Test Date	ML Algorithm					
	SVM	Neural	Log	SVM	Neural	Log
	without small leak accuracy			with small leak accuracy		
18/2/2019	75.602	78.17	67.416	52.513	50.374	47.059
20/2/2019	64.904	67.147	70.513	49.412	37.968	45.775
12/3/2019	40.385	44.444	40.812	43.077	35.769	49.744
Average	60.297	63.254	59.58	48.334	41.37	47.526

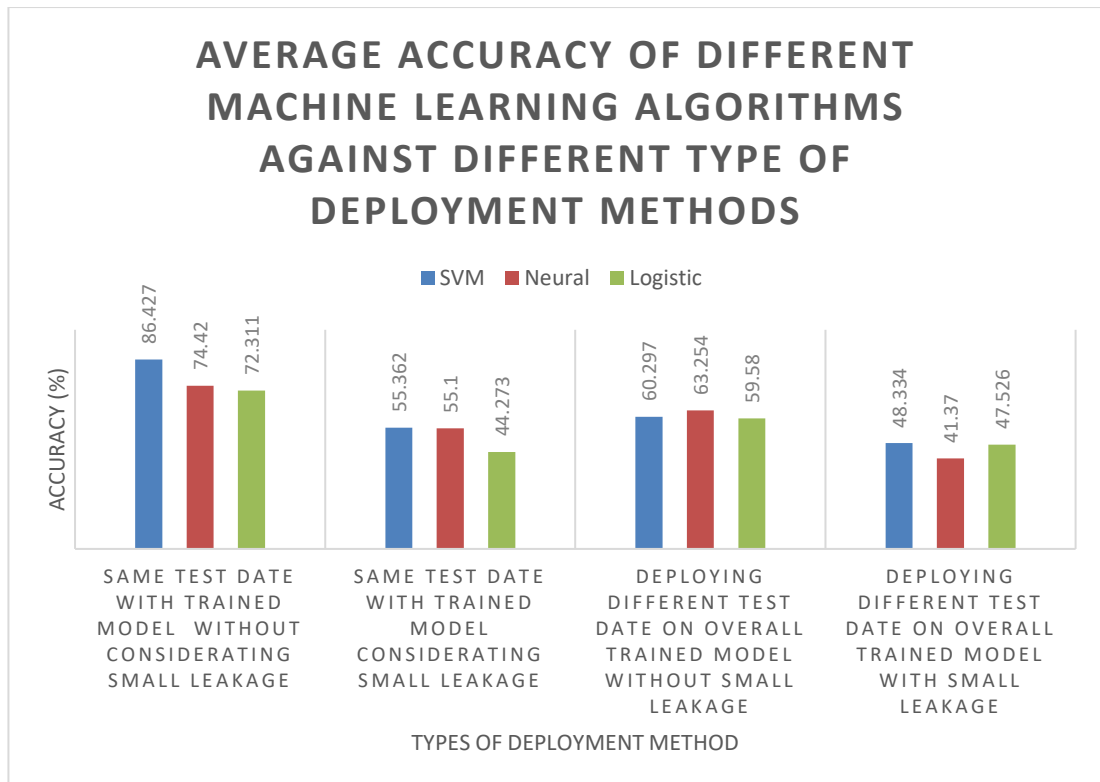


Figure 4.1: Average accuracy of different machine learning algorithms against different type of deployment methods

Based on results from Table 4.1, it can be concluded that SVM has the highest overall accuracy among these ML. Without taking the consideration of small leakage in ML, SVM has an average accuracy of 86.427% followed on by neural with 74.42% and lastly logistic with only 72.311%. Furthermore, even when including small leakage, SVM still has the highest average accuracy of 69.97% followed on by neural and also logistic. Based on Table 4.2, neural ML has the highest accuracy of around 63.254% followed by SVM 60.297% and logistic of 59.58%. when small leakage is not

considered. When small leakage is considered, the highest accuracy obtained is from SVM again which is close to half around 48.334% followed by logistic 47.526% and lastly neural 41.37%. Figure 4.1 shows a simple summary of the average accuracy from Table 4.1 and 4.2.

Table 4.3: Different test data deployed on different trained model dates (without small leakage)

Training Date	Test Data Date			Test Data Date			Test Data Date		
	18/2/2019			20/2/2019			12/3/2019		
	SVM	Neural	Log	SVM	Neural	Log	SVM	Neural	Log
18/2/2019	90.53	80.096	66.613	27.564	28.526	25	4.701	5.128	33.333
20/2/2019	26.806	30.979	12.36	89.263	85.897	74.039	17.949	23.718	10.684
12/3/2019	39.005	35.634	19.904	31.891	31.891	31.41	79.487	57.265	76.282

Table 4.4: Different test data deployed on different trained model dates (with small leakage)

Training Date	Test Data Date			Test Data Date			Test Data Date		
	18/2/2019			20/2/2019			12/3/2019		
	SVM	Neural	Log	SVM	Neural	Log	SVM	Neural	Log
18/2/2019	62.246	66.845	58.503	14.836	9.703	10.826	17.821	13.974	2.308
20/2/2019	25.134	18.075	9.626	51.403	51.403	46.752	8.333	7.949	9.872
12/3/2019	23.85	22.46	16.898	18.925	13.633	34.082	52.436	47.051	27.564

From Table 4.3 and Table 4.4, it is observed that test data deployed on different trained model dates without including its trained data of same date has remarkably low accuracy with the highest only reaching 39.005%. while the lowest can be 2.3008%.

4.3 Discussion

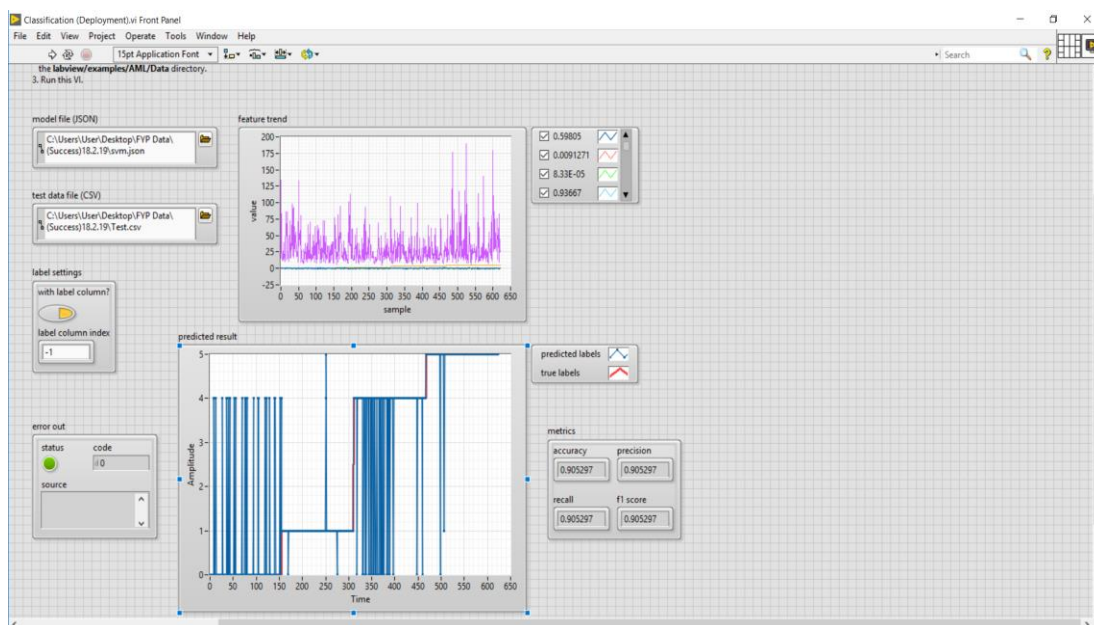


Figure 4.2: 18/2/2019 SVM model deployed on 18/2/2019 test data without small leak

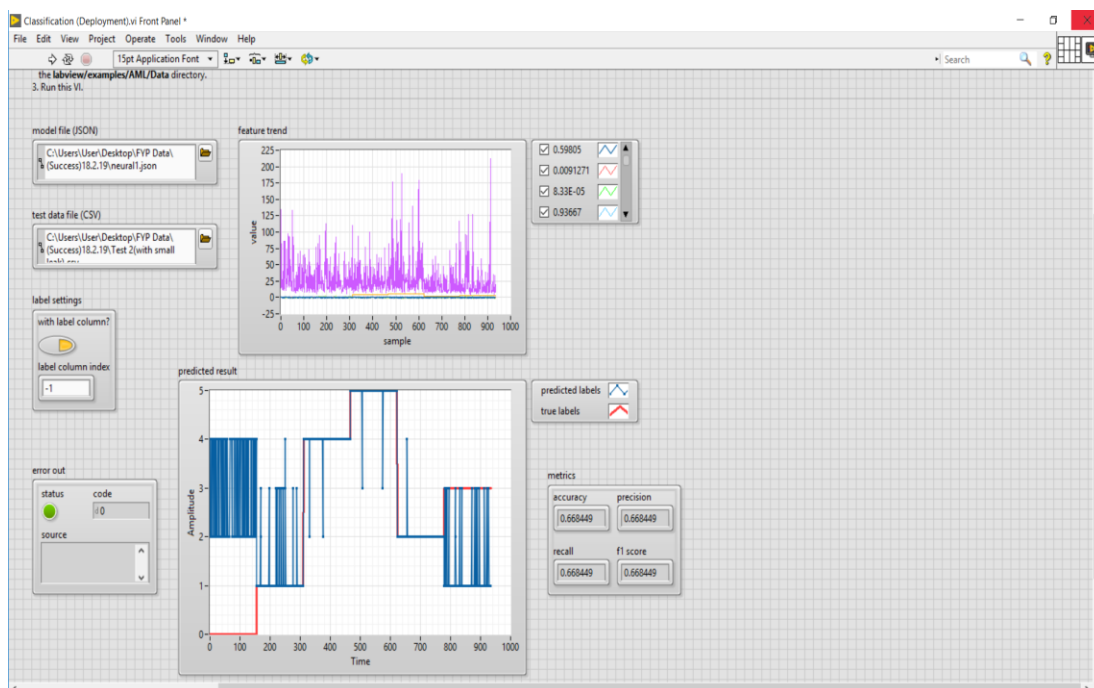


Figure 4.3: 18/2/2019 Neural model deployed on 18/2/2019 test data with small leak

Figure 4.2 and 4.3 shows the deployment of different ML algorithm on different types of data. Figure 4.2 does not include small leakage during training and deployment of the ML while Figure 4.3 includes small leakage. From Figure 4.2, it can be observed

that it has a rather high accuracy as the blue line which is the prediction of the ML algorithm matches closely with the red line. It only includes 4 categories in this case as small leakages are all exempted from this ML training and deployment. Based on Figure 4.2, it can be observed most errors occur on the sensor 1 for both no leakage and leakage conditions. Sensor 1 might have a higher error as it is closer to the wall of the building resulting in slight vibration in building affecting the accuracy of acoustic vibration collected. Figure 4.3 on the other hand shows that errors occur mostly on sensor 1: no leakage and also sensor 2: leakage condition. Predicted values are mostly on 2 or 4 for sensor 1: no leakage condition as sensor 1 is too close to the wall. Sensor 2: small leakage condition has trouble in differentiating between small leakage and no leakage as the difference in vibration might be too small to be detected. A large hissing sound and vibration sound can be heard when it is under leakage condition meanwhile small leakage only has a barely detectable hiss sound released and the vibration noticed is not that much difference as compared with no leakage condition.

Every experiment is sure to face trouble or problems and this experiment conducted is no exception. As Robert Schuller once said: "*Problems are not stop signs, they are guidelines.*" Through this experiment, it can be deduced that five types of problems were encountered.

First, uncontrolled behaviour of the building's lift system affects the overall accuracy of the data obtained. As the experiment is setup on above 10th floor, the lifts motor which is located at 10th floor is very close to the experiment setup area. When the lift in the building moves, strong vibrations are produced which can be heard. These strong vibrations pose possibility of affecting the acoustic vibration collected from the optical sensors as the pipeline system is in contact with the walls. This inconsistent vibration produced by the lift causes the experiment to collect different results each time it is conducted reducing the accuracy of data collected.

Next, constant flowrate is hard to be produced in this experiment due to the valve used. Initially, a needle valve was used in this experiment to collect data but the flowrate fluctuates around the desired value of the experiment and it is not able to reach a large leakage value. For example, when the desired value is 1 kg/hr, the flowrate reaches around 1.1-1.2 kg/hr but after a few seconds it will start to drop to about 0.1-0.2 kg/hr then rise back to 0.5-0.6 kg/hr. The inconsistent of the flowrate produces an unstable vibration resulting in an inaccurate data collected. This might be

caused by the freezing of the valve when the leakage is opened too long resulting in blockage in the valve preventing the R410 gas to be leaked.

Another issue faced in this experiment is the setting up of the experiment. The equipment needs to be installed and removed each day after the experiment in case of losing it. As the sensors are detached and reattached each time after use, there is a possibility the sensor is not attached the exact same way as on different days causing signal collected for each day to differ. This effect is observed from the power spectral density (PSD) graph as each day the sensor has a different resonance that needs to be reconfigured to 20 kHz. Basically, the condition of the experiment varies from day to day due to the setting up of experiment for each day.

One possible factor contributing to the poor accuracy in Table 4.4 might be caused by the different surrounding parameters on each day. As air conditioner produces more work done when the surrounding temperature is higher, vibration produced varies with the surrounding temperature. Surrounding humidity and air flow can also cause a different vibration produced by the pipeline as the air conditioner will try to adjust to the humidity set by the remote.

Besides, SMF sensor lacks the sufficient sensitivity required in this experiment. From the data obtained, it can be observed that the sensor fails to differentiate between the data obtained from micro leakage or small leakage to no leakage condition. The sensor has the ability and capability to differentiate between large leakages and no leakages only as it is very significance when compared to small leakage and no leakage condition.

4.4 Summary

In general, this experiment has a very high accuracy in detecting leakage condition for ML algorithm with SVM with an average accuracy of 86.427% leading followed by neural (74.42%) and lastly logistic regression (72.311%) when the trained model used is the same date as its test data obtained. When the training models of these three days are compiled together and deployed on different test date, the accuracy is around 59%-63% without considering small leakage. However, when small leakage is considered the accuracy decreases to around 41%-48%. Lastly, different trained model deployed on different test date has a very low accuracy in determining whether there is leakage or not with the highest attaining 39.005%. while the lowest 2.3008

CHAPTER 5

RECOMMENDATIONS AND CONCLUSIONS

5.1 Recommendations

Improvements that can be done to this experiment includes using a more sensitive optical sensor. From the results obtained it can be observed the sensor has a problem differentiating between no leakage condition and small leakage. This might be because the vibration produced for these cases are too similar and the sensor lacks the sufficient sensitivity to collect these data.

Another improvement for this experiment that can be done is installing a mass flow controller. This flowrate meter and sensor controls the flowrate of the leakage and ensures it is at a desired value without any fluctuation. When the flowrate exceeds or is below the desired value, it will adjust the flowrate to its desired value. A constant flowrate enables a much more precise data collected which in the end improves the overall accuracy of this experiment.

Lastly, constant and early monitoring can be done for this experiment to improve its accuracy. This experiment can start perform the monitoring of the pipeline system early and collect data of the background noise to be filtered out later. Constant monitoring should be done to accumulate the trained model of this experiment to predict the appearance of leakage or not.

5.2 Conclusion

Generally, this experiment is proven to be successful as it manages to predict and localize leakages with a very high accuracy with the highest reaching 90.53% when training model is conducted on same date with test data. When small leak is considered, the highest accuracy that can be obtained is 66% which is more than half making it quite accurate. SVM is proven to be one of the most accurate ML algorithm followed by neural and logistic regression. Accuracy of this experiment can be further improved by using a much more sensitive optic fiber and using a mass flow controller to control the flow rate of the leakage at a constant value.

REFERENCES

Anon 2013. *3 Common Causes of AC System Refrigerant Leaks*. [online] Countrysideph. Available at: <<http://countrysideph.com/blog/3-common-causes-of-ac-system-refrigerant-leaks/>> [Accessed 31 Jul. 2018].

Anon 2013. *Components of an air conditioning system*. [online] Available at: <<http://www.aceac.com/hvac-info-center/components-of-an-air-conditioning-system/>> [Accessed 16 Aug. 2018].

Anon 2017. *What Causes Refrigerant Leaks?* [online] kirkairconditioning. Available at: <<https://kirkairconditioning.us/blog/causes-refrigerant-leaks/>> [Accessed 31 Jul. 2018].

Anon 2018. *Air/Soap Test*. [online] Available at: <<https://www.pei.org/wiki/airsoap-test>> [Accessed 14 Aug. 2018].

Anon 2018. *Cable Basics: Fiber Optic Cable*. [online] Available at: <http://www.beldencables-emea.com/en/products/cable_basics/fiber-optic-cable/index.phtml> [Accessed 14 Aug. 2018].

Anon 2018. *Cross-Correlation*. [online] Mathworld. Available at: <<http://mathworld.wolfram.com/Cross-Correlation.html>> [Accessed 21 Aug. 2018].

Anon 2018. *Evaporator Coil*. [online] LENNOX. Available at: <<https://www.lennox.com/buyers-guide/guide-to-hvac/glossary/evaporator-coil>> [Accessed 16 Aug. 2018].

Anon 2018. *Negative Pressure Wave Description*. [online] PAS. Available at: <<http://www.pasmost.cz/en/leak-detection-system/npw-description>> [Accessed 18 Aug. 2018].

Anon 2018. *Piezoelectric Effect*. [online] Available at: <<http://hyperphysics.phy->

astr.gsu.edu/hbase/Solids/piezo.html> [Accessed 18 Aug. 2018].

Anon 2018. *Sending information*. [online] BBC Science and Nature. Available at: http://www.bbc.co.uk/schools/gcsebitesize/science/aqa_pre_2011/radiation/sending_rev1.shtml> [Accessed 6 Aug. 2018].

Anon 2018. *Signs And Effects Of Refrigerant Leak In Air Conditioners*. [online] Available at: <https://coolmax.sg/signs-and-effects-of-refrigerant-leak-in-air-conditioners/>> [Accessed 31 Jul. 2018].

Anon 2018. *The Purpose of Refrigerant in Air Conditioning Systems*. [online] Available at: <https://www.cleanairactheatingandac.com/blog/air-conditioning-service/the-purpose-of-refrigerant-in-air-conditioning-systems/>> [Accessed 16 Aug. 2018].

Anon 2018. *What are the Specific Advantages of FBG Sensors?* [online] Micron Optics. Available at: <http://www.micronoptics.com/what-are-the-specific-advantages-of-fbg-sensors-2/>> [Accessed 19 Aug. 2018].

Anon 2018. *What Is Data Acquisition?* [online] National Instrument. Available at: <http://www.ni.com/data-acquisition/what-is/>> [Accessed 23 Aug. 2018].

Anon 2018. *What is PZT?* [online] American Piezo. Available at: <https://www.americanpiezo.com/piezo-theory/pzt.html>> [Accessed 18 Aug. 2018].

Anon 2018. *Willis Carrier*. [online] Carrier. Available at: <https://www.carrier.com/carrier/en/us/about-carrier/willis-carrier/>> [Accessed 21 Aug. 2018].

Anon 2019. *Erbium-Doped Fiber Amplifier (EDFA)*. [online] Fiber Labs. Available at: <https://www.fiberlabs.com/glossary/erbium-doped-fiber-amplifier/>> [Accessed 17 Mar. 2019].

Anon 2019. *PIN PHOTODETECTOR CHARACTERISTICS FOR OPTICAL FIBER COMMUNICATION*. [online] FOSCO. Available at: <<https://www.fiberoptics4sale.com/blogs/archive-posts/95046662-pin-photodetector-characteristics-for-optical-fiber-communication>> [Accessed 17 Mar. 2019].

Anon 2019. *THE BASICS OF WAVELENGTH DIVISION MULTIPLEXING, WDM*. [online] Smart Optics. Available at: <<https://www.smartoptics.com/this-is-wdm/the-basics-of-wavelength-division-multiplexing-wdm/>> [Accessed 17 Mar. 2019].

Anon 2019. *What is a Fiber Bragg Grating?* [online] HBM. Available at: <<https://www.hbm.com/en/4596/what-is-a-fiber-bragg-grating/>> [Accessed 17 Mar. 2019].

AZoSensors, 2014. *What are Fiber Optic Sensors?* [online] Available at: <<https://www.azosensors.com/article.aspx?ArticleID=333>> [Accessed 6 Aug. 2018].

Baum, R., 2017. Chlorofluorocarbons and Ozone Depletion. *American Chemical Society*. [online] Available at: <<https://www.acs.org/content/dam/acsorg/education/whatischemistry/landmarks/cfcs-ozone/cfcs-ozone.pdf>>.

Brain, M., Bryant, C.W. and Elliot, S., 2018. *How Air Conditioners Work*. [online] Available at: <<https://home.howstuffworks.com/ac2.htm>> [Accessed 16 Aug. 2018].

Elandalibe, K., Jbari, A. and Bourouhou, A., 2016. Application of cross-correlation technique for multi leakage detection. *Proceedings of 2015 IEEE World Conference on Complex Systems, WCCS 2015*, 2, pp.2–5.

Fidanboyly and Efendioglu, H.S., 2009. Fiber optic sensors and their applications. *Symposium A Quarterly Journal In Modern Foreign Literatures*, [online] pp.1–6. Available at: <http://iats09.karabuk.edu.tr/press/pro/02_KeynoteAddress.pdf>.

Fukushima, K., Maeshima, R., Kinoshita, A., Shiraishi, H. and Koshijima, I., 2000. Computers & Chemical Engineering. *Computers and Chemical Engineering* 24, 24, pp.453–456.

Gao, Y., Brennan, M.J., Liu, Y., Almeida, F.C.L. and Joseph, P.F., 2017. Improving the shape of the cross-correlation function for leak detection in a plastic water distribution pipe using acoustic signals. *Applied Acoustics*, [online] 127, pp.24–33. Available at: <<http://dx.doi.org/10.1016/j.apacoust.2017.05.033>>.

Hou, Q., Ren, L., Jiao, W., Zou, P. and Song, G., 2013. An Improved Negative Pressure Wave Method for Natural Gas Pipeline Leak Location Using FBG Based Strain Sensor and Wavelet Transform. 2013.

Khemani, H. and Stonecypher, L., 2007. *Why We Need...* [online] Bright Hub Engineering. Available at: <executableoutlines.com> [Accessed 31 Jul. 2018].

Liu, C., Li, Y., Fang, L. and Xu, M., 2017. Experimental study on a de-noising system for gas and oil pipelines based on an acoustic leak detection and location method. *International Journal of Pressure Vessels and Piping*, [online] 151, pp.20–34. Available at: <<http://dx.doi.org/10.1016/j.ijpvp.2017.02.001>>.

Mishra, A., Soni, A. and Delhi, N., 2011. Leakage Detection using Fibre Optics Distributed Temperature Sensing. *6 th Pipeline Technology Conference 2011*, pp.1–12.

Omnisens, 2001. Detecting pipeline leaks using fiber optic sensing. pp.2–4.

Penner, E., Stephens, J., Odusina, E., Akingbola, J., Mannel, D. and Bagajewicz, M., n.d. Economic Comparison of a Simulator-Based GLR Method for Pipeline Leak Detection with Other Methods. [online] pp.1–29. Available at: <<https://pdfs.semanticscholar.org/df2d/f9185d95dcfc990649d068af29b4d14ba75b.pdf>>.

Post, M., 2015. 8 injured in Hammonton refrigerant leak. *The Press of Atlantic City*. [online] 29 Apr. Available at: <https://www.pressofatlanticcity.com/news/injured-in-hammonton-refrigerant-leak/article_80c91472-ee91-11e4-99b2-43f667a4e819.html> [Accessed 1 Aug. 2018].

Tian, C.H., Yan, J.C., Huang, J., Wang, Y., Kim, D.-S. and Yi, T., 2012. Negative pressure wave based pipeline Leak Detection: Challenges and algorithms. *Proceedings of 2012 IEEE International Conference on Service Operations and Logistics, and Informatics*, [online] pp.372–376. Available at: <<http://ieeexplore.ieee.org/lpdocs/epic03/wrapper.htm?arnumber=6273565>>.

Wang, J., Zhao, L., Liu, T., Li, Z., Sun, T. and Grattan, K.T.V., 2017. Novel Negative Pressure Wave-Based Pipeline Leak Detection System Using Fiber Bragg Grating-Based Pressure Sensors. *Journal of Lightwave Technology*, 35(16), pp.3366–3373.

Wang, L., Gao, X. and Liu, T., 2016. Gas pipeline small leakage feature extraction based on LMD envelope spectrum entropy and PCA-RWSVM. *Transactions of the Institute of Measurement and Control*, [online] 38(12), pp.1460–1470. Available at: <<http://dx.doi.org/10.1016/j.measurement.2014.05.012>>.

Warner Service, 2018. *Shocking Air Conditioning Statistics*. [online] Available at: <<https://blog.warnerservice.com/shocking-air-conditioning-statistics>> [Accessed 28 Jul. 2018].

Woodford, C., 2018. *Fiber optics*. [online] ExplainThatStuff. Available at: <<https://www.explainthatstuff.com/fiberoptics.html>> [Accessed 21 Aug. 2018].

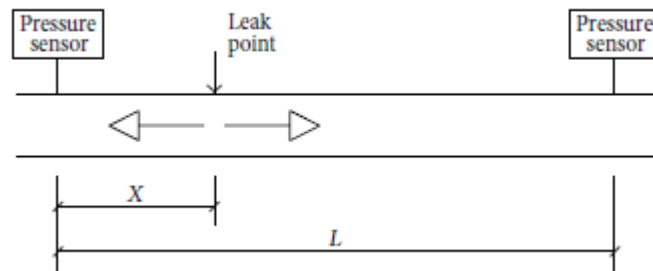
Xiao, Q., Li, J., Sun, J., Feng, H. and Jin, S., 2018. Natural-gas pipeline leak location using variational mode decomposition analysis and cross-time–frequency spectrum. *Measurement: Journal of the International Measurement Confederation*, 124(March), pp.163–172.

Xu, Q., Zhang, L. and Liang, W., 2013. Acoustic detection technology for gas pipeline leakage. *Process Safety and Environmental Protection*, [online] 91(4), pp.253–261. Available at: <<http://dx.doi.org/10.1016/j.psep.2012.05.012>>.

Zhu, J., Ren, L., Ho, S.C., Jia, Z. and Song, G., 2017. Gas pipeline leakage detection based on PZT sensors. *Smart Materials and Structures*, [online] 26(2), pp.1–7.

Available at: <<http://dx.doi.org/10.1088/1361-665X/26/2/025022>>.

APPENDICES



Appendix 1: Schematic of NPW Propagation

```

d=dir('*.*lvm');
for i=1:length(d)
    data{i}=lvm_import(d(i).name,0);
end
for i=1:length(d)

    m(i,6)=kurtosis(data{i}.Segment1.data(:,2));
    m(i,5)=skewness(data{i}.Segment1.data(:,2));
    m(i,4)=rms(data{i}.Segment1.data(:,2));
    m(i,3)=var(data{i}.Segment1.data(:,2));
    m(i,2)=std(data{i}.Segment1.data(:,2));
    m(i,1)=mean(data{i}.Segment1.data(:,2));

    [b,a]=pwelch(data{i}.Segment1.data(:,2),[],[],[],512
00);
    for j=0:79
        m(i,7+j)=b(2+10*j);
    end
end
m(:,4)=m(:,4)/max(m(:,4));
m(:,1)=m(:,1)/max(m(:,1));
csvwrite('near small leak.csv',m)
clear m
for i=1:length(d)

    m(i,6)=kurtosis(data{i}.Segment1.data(:,3));
    m(i,5)=skewness(data{i}.Segment1.data(:,3));
    m(i,4)=rms(data{i}.Segment1.data(:,3));
    m(i,3)=var(data{i}.Segment1.data(:,3));
    m(i,2)=std(data{i}.Segment1.data(:,3));
    m(i,1)=mean(data{i}.Segment1.data(:,3));

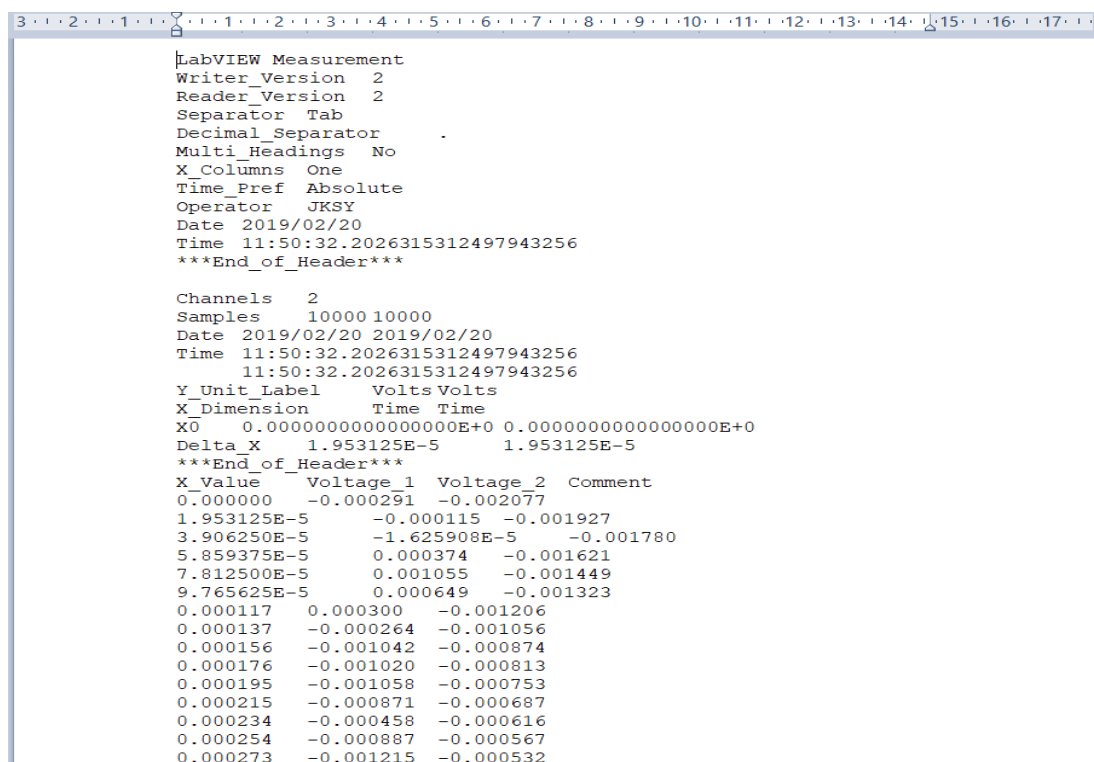
```

```

[b,a]=pwelch(data{i}.Segment1.data(:,3),[],[],[],512
00);
    for j=0:79
        m(i,7+j)=b(2+10*j);
    end
end
m(:,4)=m(:,4)./max(m(:,4));
m(:,1)=m(:,1)/max(m(:,1));
csvwrite('far small leak.csv',m)

```

Appendix 2: MATLAB code to process LVM to CSV files



```

LabVIEW Measurement
Writer_Version 2
Reader_Version 2
Separator Tab
Decimal_Separator .
Multi_Headings No
X_Columns One
Time_Pref Absolute
Operator JKSY
Date 2019/02/20
Time 11:50:32.2026315312497943256
***End_of_Header***

Channels 2
Samples 10000 10000
Date 2019/02/20 2019/02/20
Time 11:50:32.2026315312497943256
11:50:32.2026315312497943256
Y_Unit_Label Volts Volts
X_Dimension Time Time
X0 0.0000000000000000E+0 0.0000000000000000E+0
Delta X 1.953125E-5 1.953125E-5
***End_of_Header***
X_Value Voltage_1 Voltage_2 Comment
0.000000 -0.000291 -0.002077
1.953125E-5 -0.000115 -0.001927
3.906250E-5 -1.625908E-5 -0.001780
5.859375E-5 0.000374 -0.001621
7.812500E-5 0.001055 -0.001449
9.765625E-5 0.000649 -0.001323
0.000117 0.000300 -0.001206
0.000137 -0.000264 -0.001056
0.000156 -0.001042 -0.000874
0.000176 -0.001020 -0.000813
0.000195 -0.001058 -0.000753
0.000215 -0.000871 -0.000687
0.000234 -0.000458 -0.000616
0.000254 -0.000887 -0.000567
0.000273 -0.001215 -0.000532

```

Appendix 3: Sample of LVM file

